Infrared Optical Fibers

TADASHI MIYASHITA AND TOYOTAKA MANABE

(Invited Paper)

Abstract—**A state of the art review of nonsilica based infrared fibers is presented. Two types of fiber materials have been investigated—crystals and glasses. Crystal fiber work appears to be focused on development of short haul CO_2 laser power delivering lines at 10.6 μm. The maximum delivering power of the CW CO_2 laser has reached up to about 100 W by the polycrystalline KRS-5 fiber. A number of glass fibers are being developed in fluorides, sulfides, and heavy metal oxides. The best optical attenuation of each glass fiber has been respectively reduced to 21 dB/km at 2.55 μm for ZrF_4-based glass fiber with a core-clad structure, 78 dB/km at 2.4 μm for As-S unclad glass fiber, and 13 dB/km at 2.05 μm (70 dB/km at 2.40 μm) for GeO_2-Sb_2O_3 glass fiber with a core-clad structure. Recent progress of these infrared fibers offers great potential for new wavelength fiber links operating in the 2–10 μm region which have not been realized by silica-based fiber.**

I. Introduction

RECENTLY, nonsilica based infrared fiber materials have become a center of interest as candidates for the extremely low loss optical fiber materials exceeded silica glass.

Historically, nonsilica based IR fibers were already fabricated in the early 1960's for imaging-bundles, IR remote sensors, and so on, and these had losses of typically 20 000 dB/km [1]. Since the announcement in 1970 of a 20 dB/km silica-based optical fiber [2], however, no significant progress was made in the development of nonsilica-based IR fibers, while rapid advances have been made in the development of low-attenuation silica-based optical fibers. As a result of considerable progress in silica-based fiber fabrication technique, it was clarified that the intrinsic optical attenuation in silica-based fibers originates from Rayleigh scattering, IR absorption edge, and UV absorption tail, and a 0.2 dB/km silica-based fiber has been obtained experimentally in 1979 [3]. The optical attenuation value almost corresponds to the ultimate intrinsic loss value for a silica-based fiber. This means that, if lower optical attenuation fibers are needed, it is necessary to develop new infrared fiber materials which have the infrared absorption edge at longer wavelength or smaller Rayleigh scattering loss compared with silica-based glass.

In 1977–1978, Pinnow *et al.* [4], Van Uitert and Wemple [5], and Goodman [6] discussed the possibility of ultralow loss, less than 10^{-2} dB/km, for IR transmitting materials, and these discussions motivated the investigations of nonsilica-based IR fiber materials anew. Potential materials for ultralow loss fibers could be classified into the following three large groups: halides, chalcogenides, and heavy metal oxides.

Halides have been considered to have the most appropriate optical properties for ultralow loss fiber because their bandgap is large and their multiphonon absorption is located in a longer wavelength region than that for silica glass. However, familiar glass compositions had been limited to BeF_2 and $ZnCl_2$ until Poulain *et al.* discovered ZrF_4-based glasses [18]. Van Uitert and Wemple discussed BeF_2 and $ZnCl_2$ glasses for ultralow loss fiber material, and predicted their intrinsic losses could be about 10^{-2} dB/km at 1.05 μm for BeF_2 glass and about 10^{-3} dB/km around 3.5–4.0 μm for $ZnCl_2$ glass [5]. Both halide glasses were easily drawn into fiber form, but low optical attenuation has not been achieved yet.

Following Pinnow *et al.* many kinds of polycrystalline fibers, such as KRS-5 [7], KCl [8], [9], NaCl [9], CsI [8], KBr [9], AgCl [10], etc., were fabricated by the extrusion method and their optical attenuations were reported. While the lowest optical absorption loss for halide crystals was measured with a bulk KCl single crystal by a laser calorimetry method [73], the lowest optical attenuation for halide polycrystalline fibers has been 300 dB/km, which was achieved with KRS-5 at 10.6 μm wavelength in 1978 by Gentile *et al.* [7]. Recently, scattering loss [11] and weak absorption tail [12] in halide crystals have been studied, but no more advances have been made in reducing optical attenuation of polycrystalline halide fibers. On the other hand, short haul applications at 10.6 μm have been considerably studied, and CO_2 laser power transmitting capabilities of polycrystalline KRS-5 fiber with 1 mm diameter have increased up to about 100 W [13] and a 10 m long polycrystalline KRS-5 fiber has been fabricated with a loss of 1.0 dB/m [14].

Some efforts have also been made in devising single crystal fiber fabrication. The single crystalline fiber was first reported with KCl in 1973 [76], and after the suggestion by Goodman in 1978 [6], a few kinds of single crystal fibers, such as AgBr [15], KRS-5 [16], CsBr [17], CsI [17], etc., have been fabricated. Logically, perfect single crystal fiber is the ideal form for the ultralow loss fiber. However, practically, the lowest optical loss for halide single crystal fibers has been 5000 dB/km, which was measured with a single crystal CsBr fiber at 10.6 μm [17], and the loss value has been larger than that of KRS-5 polycrystalline fibers. While single crystal fibers themselves would be useful in the active fiber devices such as a fiber laser, some breakthrough is required in the single crystal

Manuscript received April 1, 1982; revised June 8, 1982.

The authors are with the Ibaraki Electrical Communication Laboratory, Nippon Telegraph and Telephone Public Corporation, Tokai, Ibaraki, Japan.

0018-9480/82/1000-1420$00.75

fiber fabrication techniques to prepare ultralow loss fibers.

Since ZrF_4-based glasses were discovered by Poulain *et al.* in 1975 [18], considerable progress has been made on the BeF_2 free fluoride glasses in the improvement of glass stability, the characteristics of optical and thermal properties, and in fiber drawing techniques.

Fluoride glass compositions for IR fiber material have been focused on multicomponent glasses based on ZrF_4, HfF_4, and AlF_3. The minimum loss for ZrF_4-, HfF_4-, and AlF_3-based glasses was predicted as 10^{-2}-10^{-3} dB/km around the 2-5 μm wavelength region [19], [20]. The zero material dispersion point occurs around 1.6-1.7 μm for ZrF_4- and HfF_4-based glasses and at 1.48 μm for an AlF_3-based glass [21]-[24]. The impurity absorption losses in ZrF_4-based glass were also determined quantitatively and it was shown that the absorption intensities for transition metal ions and rare earth ions would be relatively weak in the 2-5 μm wavelength region [25], [26].

A fluoride glass fiber was first fabricated by the rod drawing technique in 1980 [27] and remarkable progress has been made in reducing fiber loss. Mitachi *et al.* have broken through some barriers for fabrication of ZrF_4-BaF_2-GdF_3 glass fibers, improving the glass stability against crystallization [28], adopting Teflon FEP coating [28], and developing a build-in casting technique to form a core-cladding structure [29]. They have recently succeeded in preparing a 21 dB/km fiber [30].

The other fluoride glass fibers have been drawn continuously with AlF_3-based [31] and ZrF_4 (or HfF_4)-BaF_2-LaF_3-based multicomponent glasses by rod drawing and crucible drawing techniques [32], [33], respectively. Remarkable advances have been made in developing new glass compositions with improved glass stability as well as with increased viscosity near the drawing temperature. Although lower loss values than 100 dB/km have not yet been obtained in these glass fibers, these new glasses may lead to applications such as laser windows, housings, and short haul IR transmission lines for the 2-5 μm region because their fabrication is relatively easy.

Chalcogenide glasses, such as Ge-S [34], As-S [35], As-Se [35], etc., have also been studied again for infrared fiber materials. Sulfide glasses are predicted to have the losses in the 10^{-2} dB/km range [34], [35], and an uncladded As-S glass fiber with the loss of 78 dB/km has already been fabricated [36]. Comparing fluoride glasses, the advantages of chalcogenide glasses are that their crystallization rate is relatively slow and homogeneous longer fiber is easily fabricated, and that their infrared absorption edge lies in longer wavelength.

Recently, GeO_2-Sb_2O_3 glass fiber was prepared by the VAD method [37]. The predicted minimum loss for GeO_2 glass is in the 0.1 dB/km range and extremely lower loss than silica fiber could not be expected, but useful applications around the 2 μm band can be expected.

Recent progress of a new family of nonsilica-based IR fiber materials offers great potential for ultralong repeaterless fiber links and short haul applications, such as IR remote sensors, IR power transmission lines, IR windows, etc., will be practically advanced.

This paper presents a state of the art review on infrared optical fibers. Particular attention is paid to fiber materials and fiber fabrication techniques, their optical characteristics, and some applications.

II. Materials

The most important criteria in the selection of an infrared fiber material are that it could be formed into a homogeneous fiber of considerable length and that it would have low optical loss potential. The materials used for the production of infrared fibers fall into two categories—glass and crystal. Glass materials are, in general, suitable for the fabrication of the practical fiber, although a suitable composition should be selected to form sufficiently stable glass without devitrification during the fiber fabrication process, especially the fiber drawing process. Crystalline materials from which fiber could be practically prepared are limited to certain families of crystals. One kind of these materials is a crystal that has great ductility and could be processed in solid state. The other kind of material for fiber is a crystal that could be grown from melt phase or from vapor phase.

Fig. 1 shows schematic optical attenuation mechanisms in fibers. Optical attenuation consists of absorption and scattering, which are classified into extrinsic and intrinsic factors. Extrinsic absorption losses originate from impurities, such as transition metal ions, rare earth metal ions, and OH ions. Extrinsic scattering losses are caused by such imperfections as bubble, stria, microcrystal, and core-cladding boundary fluctuation, which mostly depend on fiber fabrication conditions. Intrinsic losses are composed of ultraviolet and infrared absorptions, as well as Rayleigh scattering.

If the impurities are eliminated by purification and if the defects mentioned above are sufficiently minimized, then only the intrinsic loss mechanisms would remain. Inherent optical loss α_i can be written as

$$\alpha_i = \frac{A}{\lambda^4} + B_1 e^{B_2/\lambda} + C_1 e^{-C_2/\lambda}. \quad (1)$$

Here, coefficients of A, B_1, B_2, C_1, and C_2 are the constants and λ is wavelength. The first term shows Rayleigh scattering loss, and the second and the third terms show ultraviolet and infrared absorptions, respectively. The ultraviolet absorption originates from the electronic bandgap transitions and Rayleigh scattering is caused by microfluctuation in the refractive index. These two factors decrease with increasing wavelength. On the other hand, the infrared absorption, which is due to multiphonon absorption, increases with wavelength. Spectral loss in fiber is given by the superposition of these mechanisms.

As is illustrated in Fig. 1, in general, the materials would possess valley type transmission characteristics if the extrinsic factors were satisfactorily suppressed. The level at the bottom of the valley, therefore, depends on the slopes and separation of these three inherent factors.

The major criterion in the choice of material having low loss in the infrared wavelength region is that the infrared absorption band should be located at a sufficiently long wavelength. The Szigeti equation on the fundamental phonon frequency indicates that heavier ions and weaker bonding forces are preferable for a wide and deep valley of optical transmission in the infrared region [38].

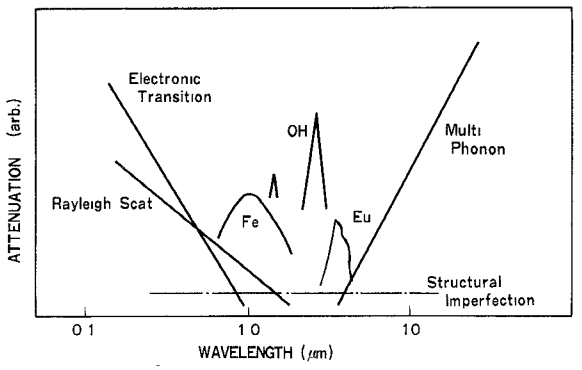

Fig. 1. Schematic optical attenuation mechanisms in fibers.

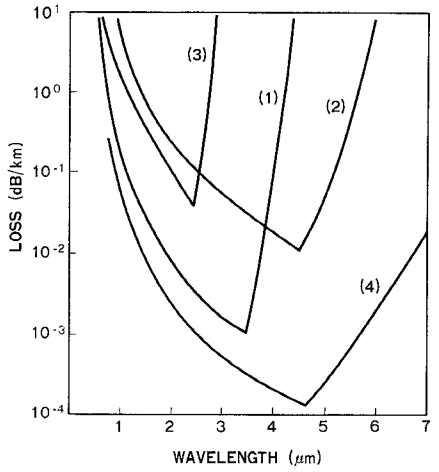

Fig. 2. Calculated loss spectra for various materials. (1) Halide glass (ZrF_4-BaF_2-GdF_3) [19]. (2) Chalcogenide glass (GeS) [19]. (3) Heavy metal oxide glass (GeO_2) [39]. (4) Crystal (KCl) [40].

Fig. 2 illustrates the calculated loss spectra for fibers made from the following four groups of candidate materials for infrared use: halide, chalcogenide, and heavy metal oxide glasses, and a halide crystal. Each term in (1) can be determined based on the empirical data on bulk materials, or by calculation using a theoretical model. As is shown in Fig. 2, the oxide glass has a relatively narrow transmission band and will not exhibit ultralow loss. Fluoride glasses have ultralow loss potential at the 2-4 μm band and chalcogenide glasses, for example, germanium-sulfide glasses have a longer cutoff wavelength than the former two groups. Halide crystalline fiber exhibits significantly low loss and wide transmission band if there were no defects giving rise to additional states within the bandgap. In addition to the feasibility of fiber fabrication and low optical loss potential, the selection of materials for IR fiber must also take into consideration other properties, e.g., chemical stability including durability and mechanical strength.

The relative merits of the various materials, which have been investigated for infrared fiber, should be evaluated in the course of developmental research in the future.

A. Halide Glasses

Table I lists halide glasses which were drawn into fibers and investigated in regard to their optical properties up to date. Halide glasses fall into two categories. The first consists of fluoride glasses and the second consists of chloride glasses. Fluoride glasses have been prepared based on a variety of glass-formers, including BeF_2, ZrF_4, and HfF_4 as well as binary systems such as AlF_3-BaF_2.

TABLE I
TYPICAL HALIDE GLASSES FOR INFRARED FIBERS

Composition	Fiber type	Reference
$BeF_2(40)$-$MgF_2(20)$-$SrF_2(20)$-$AlF_3(20)$	unclad	41
$ZrF_4(61.8)$-$BaF_2(32.3)$-$GdF_3(3.9)$-$AlF_3(2)$	clad	29
$ZrF_4(60)$-$BaF_2(31)$-$GdF_3(4)$-$LaF_3(1)$-$AlF_3(2.5)$-$PbF_2(1.5)$	*	50
$ZrF_4(57)$-$BaF_2(34)$-$LaF_3(5)$-$AlF_3(4)$	*	63
$ZrF_4(57.5)$-$BaF_2(33.5)$-$LaF_3(5.5)$-$AlF_3(3.5)$	unclad	33
$ZrF_4(57)$-$BaF_2(36)$-$LaF_3(3)$-$AlF_3(4)$	unclad	32
$ZrF_4(51)$-$BaF_2(16)$-$LaF_3(5)$-$LiF(20)$-$AlF_3(3)$-$PbF_2(5)$	unclad	44
$ZrF_4(58)$-$BaF_2(15)$-$LaF_3(6)$-$AlF_3(4)$-$NaF(21)$	unclad	45
$ZrF_4(62)$-$BaF_2(33)$-$ThF_4(5)$	*	24
$ZrF_4(60)$-$BaF_2(33)$-$ThF_4(7)$	*	11
$ZrF_4(57.5)$-$BaF_2(33.7)$-$ThF_4(8.8)$	*	10
$HfF_4(62)$-$BaF_2(33)$-$LaF_3(5)$	*	24
$HfF_4(58)$-$BaF_2(33)$-$ThF_4(9)$	*	24
$HfF_4(62)$-$BaF_2(15)$-$LaF_3(5)$-$AlF_3(2)$-$PbF_2(10)$-$CsF(6)$	plastic clad	32
$AlF_3(43)$-$BaF_2(20)$-$CaF_2(20)$-$YF_3(17)$	unclad	41
$ZnF_2(29)$-$BaF_2(20)$-$ThF_4(22.2)$-$YF_3(14.4)$-$AlF_3(14.4)$	*	63
$ZnCl_2$	unclad	5
$BiCl_3$-KCl	*	48

* not reported on fiber drawing

BeF_2 based glasses were identified over 50 years ago and extensive studies were performed on glass formation and optical properties. BeF_2, like SiO_2, easily forms a glass on cooling from the molten state and has unique optical dispersion. In spite of these potentially attractive properties, few trials of making fiber from fluoroberyllate glasses have been carried out except for the BeF_2-SrF_2-MgF_2-AlF_3 glass system [41] because the materials are highly toxic and too hygroscopic for practical handling and use.

A family of glasses based on the heavy metal fluorides has been developed by Lucas, Poulain, and co-workers [18]. Since their discovery in 1975, extensive studies have shown that these glasses can be considered as promising candidates for infrared technology. The glasses generally contain 60-70 mole% ZrF_4 as the primary constituent and 30 mole% BaF_2 as a network modifier with a small amount of another metal fluoride, like ThF_4 or rare earth fluoride, playing the role of the glass stabilizer.

The ZrF_4 based glasses are low melting materials; the crystallization, fusion, and glass transition temperatures are in the 370-450°C, 550-600°C, and about 330°C ranges, respectively. The thermal expansion coefficient is rather high, about 170×10^{-7}/°C. The refractive index(n_D) is about 1.52.

It must be noted that, in these multicomponent fluoride glasses, the composition can be readily and extensively varied

by substituting for the third constituent another rare earth element or actinides, or alkali fluoride, or even by adding fluorides like NaF, LiF, AlF_3, and PbF_2. The versatility of these systems provides a handle of some of the physical properties of the materials, which is indispensible to fiber fabrication. The differences between crystallization temperatures and T_g, which are indicative of the stability for these glasses, are generally between 70-100°C.

Glass forming region and various properties are described below in the ZrF_4-based system, particularly with respect to the ZrF_4-BaF_2-GdF_3 system, which provides the most preferable material for low-loss fiber [42]. Fig. 3 shows the glass forming and fiber drawing regions in the ZrF_4-BaF_2-GdF_3 system. The GdF_3 containing system has a larger glass forming area than other rare earth fluorides containing systems. The fiber-drawing region was defined by drawing homogeneous fiber without devitrification by a conventional preform method. Fig. 4 shows a DTA curve for the ZrF_4-BaF_2-GdF_3 glass. Glass transition temperature T_g and crystallization temperature T_x are 310 and 376°C, respectively. Deformation temperature T_d is determined as 332°C by TMA. Thermal expansion coefficients varied from 146 to 206 ($\times 10^{-7}$/°C) for the ZrF_4-BaF_2-GdF_3 glass forming region. Since the fluorozirconate glasses contain only cations of large mass number, their density is quite high, with 4.6 g/cm^3.

Table II summarizes the physical properties for ZrF_4-BaF_2-GdF_3 glass. The refractive index(n_D) is typically in the neighborhood of 1.52. It is noted that refractive index varies little according to base glass composition change. This means that some dopants are required to be added into the base glass for controlling refractive index. Fig. 5 shows the relations between dopant concentrations and refractive indexes in the ZrF_4(63)-BaF_2(33)-GdF_3(4) system [42]. PbF_2 and BiF_3 increase the refractive indexes. On the other hand, LiF, NaF, and AlF_3 decrease the refractive indexes. Among these materials, AlF_3 is found to be the most preferable dopant for forming a core cladding refractive index profile from the point of view of thermal behaviors such as expansion coefficient and deformation point.

A typical transmission spectrum for a bulk sample is shown in Fig. 6 for ZrF_4-BaF_2-GdF_3. The optical transparency interval for 50 percent transmittance is about 0.23–7 μm with no other absorption bands between these limits. The wide IR transparency for fluorozirconate glasses is clearly related to a large mass of the component elements and a correspondingly small value of the bond force constants. The fiber is fabricated from the base glass composed of ZrF_4(63)-BaF_2(33)-GdF_3(4), which is located at the center of the fiber-forming region, as shown in Fig. 3.

ZrF_4-based glass, containing other metal fluorides like LaF_3 and ThF_4, have been extensively investigated [24], [32], [33], [44], [45]. Many research efforts have been carried out on a variety of these glasses, covering subjects such as glass preparation, viscosity, thermal properties, UV and IR absorptions, dispersive properties, and fiber fabrication.

Fiber drawing often leads to devitrification, which is largely due to a narrow working range and a steep viscosity-tempera-

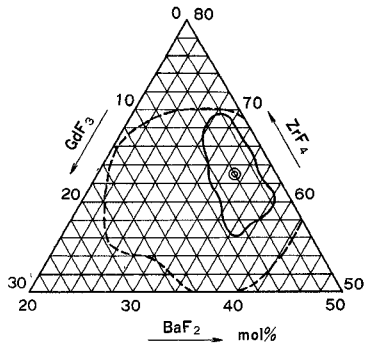

Fig. 3. Glass forming and fiber drawing regions in the ZrF_4-BaF_2-GdF_3 system. ⊙: Composition used for fiber drawing.

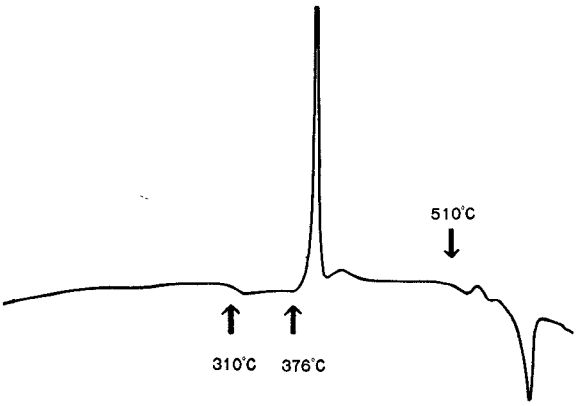

Fig. 4. A differential thermal analysis curve for the ZrF_4-BaF_2-GdF_3 glass.

TABLE II
OPTICAL AND THERMOMECHANICAL PROPERTIES IN ZrF_4(63)-BaF_2(33)-GdF_3(4) GLASS

Transmission range (μm)	0.23 - 7.0 (4mm thick)
Refractive index (n_D)	1.529
Thermal expansion coefficient(°C^{-1})	175 x 10^{-7}
Glass transition temperature(°C)	310
Deformation temperature(°C)	332
Crystallization temperature(°C)	376
Density(g.cm^{-3})	4.6

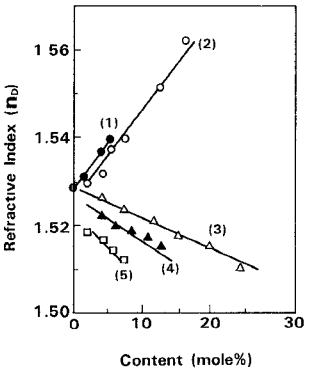

Fig. 5. The relations between dopant concentration and refractive index in the ZrF_4(63)-BaF_2(33)-GdF_3(4) system. (1) PbF_2. (2) BiF_3. (3) LiF. (4) NaF. (5) AlF_3.

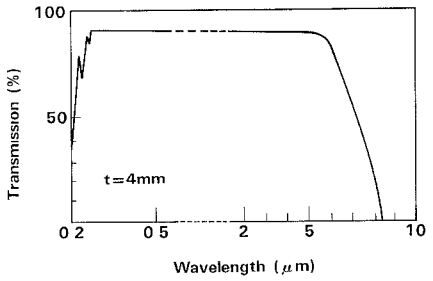

Fig. 6. Optical transmission in the ZrF_4-BaF_2-GdF_3 glass.

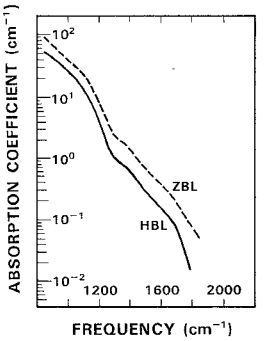

Fig. 7. Multiphonon absorption coefficients for fluoride glasses [24]. ZBL: ZrF_4-BaF_2-LaF_3 system. HBL: HfF_4-BaF_2-LaF_3 system.

ture relation. Improvement in glass stability is the basic problem to be solved for preparing high quality fiber. Attempts on improvement in glass stability are taken by doping additives into the base composition. Alkali fluorides such as LiF and NaF, AlF_3, and PbF_2 are found to be useful for suppression of devitrification or for extension of glass working range. ZrF_4(57)-BaF_2(36)-LaF_3(3)-AlF_3(4) composition glasses were provided for fiber fabrication by the crucible technique [32] in which the crucible apparatus was specially designed for avoiding devitrification during the drawing process. Multimeter lengths of uncladded fiber have been prepared, while no detailed evaluation has yet been reported in terms of optical attenuation. The PbF_2 doped ZrF_4-BaF_2-LaF_3-AlF_3-LiF glass enables drawing fibers reaching 1 km by a conventional crucible technique [44]. The NaF doped ZrF_4(58)-BaF_2(15)-LaF_3(6)-AlF_3(4) was also provided for fiber fabrication [45]. A family of ZrF_4-based glass substituting LaF_3 or GdF_3 by ThF_4 was developed [10], [11], [24]. However, fiber drawing has not been reported yet.

Glasses based on heavier HfF_4, which is virtually chemically identical to ZrF_4, were studied. These glasses are transparent out to longer wavelengths than the corresponding ZrF_4-based glasses [24]. Thus, at a certain wavelength, the absorption coefficient for HfF_4-based glass should be lower than that for an analogous ZrF_4-based glass. As is shown in Fig. 7, the multiphonon absorption edges for HfF_4-based glasses were shifted to longer wavelengths with respect to the ZrF_4-based glasses. Plastic clad fiber was prepared using HfF_4(62)-BaF_2(15)-LaF_3(5)-AlF_3(2)-PbF_2(10)-CsF(6) glass, but there have been few data on optical attenuation in the drawn fiber [32].

A number of multicomponent fluoride glass systems with ZrF_4 and HfF_4 free compositions have been reported, including ZnF_2/ThF_4 [46], BaF_2/ThF_4 [24], BaF_2/ZnF_2 [63] compositions, and the AlF_3-based system [31]. These glasses, however, are less stable than ZrF_4- and HfF_4-based glasses, and are not yet drawn into fibers, except for the AlF_3-based system. Using the AlF_3(43)-BaF_2(20)-CaF_2(20)-YF_3(17) composition, unclad fibers were prepared by the rod drawing technique [41]. Although the minimum loss was obtained with 100 dB/km at 2.5 μm in the AlF_3-based glass fiber, it might be very difficult to reduce transmission loss further because of devitrification occuring during the fiber drawing process.

Chloride glasses would be alternate candidates for IR glass fibers, although they are too hygroscopic for practical handling. Only $ZnCl_2$ was drawn into the unclad fiber by the crucible technique, but its optical loss characteristics have not been measured [5]. Glass formation in the $BiCl_3$-KCl system has also been reported [48].

B. Chalcogenide Glasses

Chalcogenide glasses containing the elements As, Ge, P and S, Se, and Te are available with a stable vitreous state and a wide transmission range [47]. Many research projects on fabrication process, optical properties, and physical and chemical characteristics have been undertaken for several varieties of chalcogenide glasses. Chalcogenide glasses have a large glass forming area, stability against moisture, larger refractive index, and longer cutoff wavelength compared with fluoride and oxide glasses. Some of the glasses are widely used for infrared applications such as window materials and optical devices for CO_2 laser wavelength. However, there is yet little information available on fiber fabrication with the chalcogenide glasses.

Table III lists typical chalcogenide materials from which fiber has been fabricated up to date. The arsenic-sulphur glasses are one of the most practical choices of chalcogenide glasses for infrared fiber optics. Variations of arsenic-sulphur glass systems are easily available, which have the necessary physical properties for the fabrication of clad type fibers with suitable numerical apertures. This glass has a softening point of 205°C and a thermal expansion coefficient of $250(\times 10^{-7}/°C)$. It gives a fairly broad range of transmission between 0.6 and 10 μm (10 mm thick) and has a relatively high refractive index of 2.41.

From the arsenic-sulphur glasses, fibers were first prepared by Kapany and Simms, which showed relatively high optical loss of 20 dB/m at 5.5 μm wavelength [1]. Recently, unclad fibers were drawn from the As_2S_3 rod [36] and clad type fibers were also prepared by a double crucible technique using $As_{38}S_{62}$ glass as a core and $As_{35}S_{65}$ as a cladding [49]. It is noted that arsenic-sulphur glass has a tendency toward devitrification during fiber fabrication process, depending on the drawing technique. Fig. 8 illustrates composition ranges which can be drawn into fiber by the preform and the crucible techniques. Arsenic-selenide glass has a longer cutoff wavelength than arsenic-sulfide glass. A combination of As_2Se_3 as a core and As_2S_3 as a cladding was used for fiber preparation [35].

A second group of chalcogenide glass, which was studied for use as a fiber material, is germanium-sulfide glass [34], [52], [53]. It has relatively higher softening temperature, large

TABLE III
TYPICAL CHALCOGENIDE GLASSES FOR INFRARED FIBERS

Composition	Fiber type	Reference
As_2S_3	unclad, clad	1, 36
$As_{38}S_{62}$ - $As_{35}S_{65}$	clad	49
As_2Se_3	unclad	51
As_2Se_3 - As_2S_3	clad	35
GeS_3	unclad,plastic clad	53, 52
$Ge_3PS_{7.5}$	unclad	34
$Ge_{30}As_{15}Se_{55}$	unclad	54
La-Ga-Ge-Se	*	55

* not reported on fiber drawing

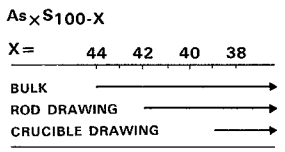

Fig. 8. Fiber drawing regions in As-S system by preform and crucible techniques.

glass forming area, and low toxicity. Fig. 9 shows glass forming and fiber-drawing compositions for the Ge-P-S glass system. The latter is narrower as compared with the former because of devitrification in the Ge rich region and sublimation of sulphur in the S rich region at a temperature above the softening point. The appropriate glass composition in Ge-S system for drawing fibers is limited to composition GeS_x, where x ranges from 2 to 4. Addition of phosphorous to the germanium sulfide glass increases glass forming ability and optical homogeneity if the amount of phosphorous was less than 10 mole%.

Table IV lists the physical properties of GeS_3 glass. Physical properties strongly depend on the glass compositions; T_g, T_d, T_x, and Knoop hardness decrease with increasing sulphur (or phosphorus) content. The optical transmission range for germanium-sulphur glass is almost identical to that for arsenic-sulphur glass, giving a broad transmission between 0.5 and 11 μm (2 mm thickness). Germanium-sulphur glasses have a relatively low refractive index (n_D) of about 2.1 among chalcogenide glasses, which is favorable for low loss because Rayleigh scattering loss is proportional to n^8. Unclad and silicone clad fibers have been drawn from $GeS_{2.2}$, GeS_3, and $Ge_3PS_{7.5}$ glasses.

Among varieties of selenide glasses, $Ge_{30}As_{15}Se_{55}$ glass was used for preparing fiber [54] and the La-Ga-Ge-Se system is also known to be highly transparent in the infrared region [55].

C. Oxide Glasses

Some heavy metal oxide glasses can transmit the longer wavelength light beyond 2 μm. Typical glasses for midinfrared transmission are La_2O_3, GeO_2 and TeO_2 based glasses, and $CaO\text{-}Al_2O_3$ glass [56]. However, the materials from which long fibers were drawn and whose fiber properties were examined have been limited to only a few glasses. Table V lists typical heavy metal oxide glasses for infrared fibers.

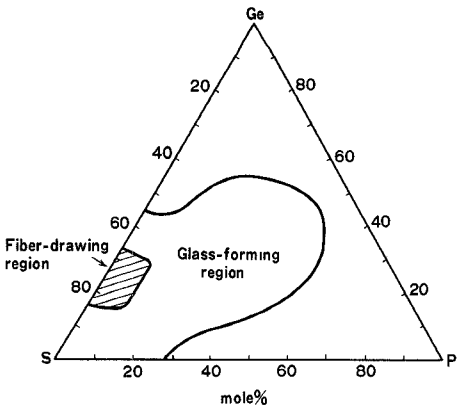

Fig. 9. Glass forming and fiber drawing regions for Ge-P-S system.

TABLE IV
OPTICAL AND THERMOMECHANICAL PROPERTIES IN GeS_3 GLASS

Transmission range (μm)	0.5 - 11
Refractive index (n_D)	2.113
Thermal expansion coefficient	250 x 10^{-7}
Glass transition temperature (°C)	260
Deformation temperature (°C)	340
Crystallization temperature (°C)	500
Density (g.cm^{-3})	2.5

TABLE V
TYPICAL OXIDE GLASSES FOR INFRARED FIBERS

Composition	Fiber type	Reference
GeO_2-Sb_2O_5	clad	37, 64
TeO_2(70)-ZnO(20)-BaO(10)	unclad	54

Although a lanthanate glass was selected for the 0.4–5 μm infrared fiber optics 20 years ago [1], details on fiber fabrication and its optical properties have not been described. The feasibility of using GeO_2 as the base glass for fiber has been known for several years. Recently, germanate glass was suggested to be useful for infrared fiber with a minimum loss of less than 0.2 dB/km at 2.5 μm and zero material dispersion of near 1.69 μm [39]. Germanate glass has been synthesized by the vapor-phase axial deposition (VAD) method [37], which was developed for preparing high silica glass fiber preforms. Antimony was doped into the base GeO_2 for stabilizing the vitreous state and for controlling the refractive index profile. Germanate glasses have a cutoff wavelength of about 5 μm for a 2 mm thick sample. No absorption can be found near 3 μm due to OH for the glass prepared by the VAD method while a large amount of OH is usually contained for glass prepared by the crucible technique. The refractive index for the germanate glass increases almost linearly with an increase in antimony content. Long lengths of fiber reaching 400 m were successfully prepared from the GeO_2-Sb_2O_3 glass.

Tellurium oxide-based glasses have been prepared for IR fibers. TeO_2-WO_3-Ta_2O_5, TeO_2-WO_3-Bi_2O_3, TeO_2-BaO-ZnO, and TeO_2-BaO-PbO glass systems were studied on glass forming region, absorption spectra, and refractive indexes [54]. The TeO_2-ZnO-BaO has a cutoff of 6 μm in the infrared wavelength

region for 5 mm thick plate and a refractive index of 2.0. From these glasses, which were prepared by a dehydration process, fibers were made 200 μm in diameter and spectral loss measurements were carried out from 0.5 to 12 μm.

D. Crystal

Halide materials are a logical choice since the fundamental phonon absorption bands are located in the far infrared. The optical transparency of these materials covers a much broader spectral range than those of other IR materials. Transmission wavelength band extends from approximately 0.13 μm in the UV to 35 μm in the IR range. Theoretical calculations indicate the superiority of halide crystals as fiber materials with predicted losses as low as 10^{-3} dB/km, or lower than that at selected near infrared wavelengths [4]. Some of halide materials also possess suitable mechanical and physical properties to allow fiber fabrication.

Table VI lists typical halide crystals from which fibers have been made. They are segregated into two categories: polycrystal and single crystal. In general, the former fiber can be extruded from a solid and the latter fiber is grown from a melt.

KRS-5(TlBrI) has been most extensively investigated for IR fiber since the first announcement in 1977 by Pinnow *et al.* at Hughes Research Laboratories [4]. KRS-5 is superior in mechanical and chemical properties to other crystals for IR fiber. KRS-5 has a melting point of 415°C which is relatively low compared with other alkali halides and has a high tensile strength of 3.8 kg/mm^2. It has some solubility in water around 5×10^{-2} g in 100 g H_2O. KRS-5 is transparent from 0.63 μm in the visible to 35 μm in the infrared. Minimum loss is calculated to be 10^{-3} dB/km at 7.0 μm. Its transparency decreases gradually in the shorter wavelength region. Refractive index for this material is 2.37 at 10.6 μm. Only unclad or loose plastic clad fibers have been prepared from KRS-5. Crystalline cladding has not been achieved, although some attempts at TlBr cladding on the KRS-5 core have been tried.

KRS-6(TlBrCl) and TlBr which have similar properties to KRS-5 are also used for IR fiber. However, these materials have the inferiority of relatively high solubility in water.

The silver halide (AgBr) also has a low melting point of 449°C, very little solubility in water of 3×10^{-4} g per 100 g H_2O(25°C), and a refractive index of 1.98. Because of their great ductility, the silver halides have been successfully extruded into polycrystalline fiber with continuous length up to 200 m [10].

Recently, single crystalline fibers have also been grown from KRS-5 and AgBr [15], [16], respectively. These fibers offer alternatives to the polycrystalline fibers because they would not have scattering centers associated with grain boundaries in polycrystal fibers. Alkali halides such as KCl, CsBr, and CsI are used for fabrication of crystalline fiber, mostly single crystal fiber [11], [17], [59] because it is very difficult to form these materials into fiber by extrusion techniques because of their high solubility and high melting points. One attempt has been tried to extrude KCl; however, it was found that the surface quality for KCl fiber extruded was very poor, which results from friction between the KCl and the extrusion die because KCl readily forms microcleavage cracks [60].

TABLE VI
TYPICAL CRYSTALLINE MATERIALS FOR INFRARED FIBERS

Composition	Fiber type	Reference
KRS-5 (TlBrI)		
poly	plastic loose clad	4,7,13
single	unclad	16
TlBr		
poly	plastic loose clad	7
AgCl		
poly	unclad	10
AgBr		
poly	plastic loose clad	7,10
single	unclad	15
KCl		
poly	unclad	60
single	unclad	11
CsBr		
single	plastic loose clad	17
CsI		
single	plastic loose clad	59

CsI with a melting point of 621°C has been used for growth of single crystalline fiber and its optical attenuation has been measured in the 0.63–10.6 μm wavelength range. Absorption losses for other alkali halides such as NaCl, KBr, and CsBr have been measured on bulk materials and it was suggested that a weak absorption tail except for Urbach edge would exist and would determine the loss value [74]. However, the mechanism of the weak absorption tail observed in alkali halide crystals has not been clarified as yet, even if it originates from some intrinsic or extrinsic defects.

III. FIBER FABRICATION PROCESS

The fiber fabrication process, in general, consists of two steps: the preparation of bulk material and the formation of a thin and long fiber from the bulk. There are many variations in the bulk preparation and fiber formation processes. There is also considerable difference in fabrication processes between glass and crystalline fibers. The two basic processes, e.g., preform and crucible techniques are extensively used in glass fiber fabrication. On the other hand, crystalline fibers are prepared by extrusion techniques which are widely used in plastic and metal cable industries, and by crystal growth techniques based on the edge-defined film-fed growth (EFG) technique.

A. Fluoride Glass Fiber

Two methods have been used for fabricating fluoride glass fibers. The first involves preform fabrication, which is carried out by a casting process, and the second is the crucible technique, which would be modified for the present purpose. These two processes each have their advantages and their disadvantages, respectively. The former technique is carried out at relatively low temperatures and materials are thermally reworked at low viscosity and at a temperature far from the crystallization temperature, although it is difficult to form a smooth interface between core and cladding. On the other hand, in the latter technique, fiber formation is carried out at a considerably high temperature and the material tends to

crystallize during the drawing process. A core-cladding structure will be easily formed by the crucible technique, if the viscosity is sufficiently increased at the drawing temperature.

The preform method, in which a novel technique had to be developed to form a core-cladding structure [29], is used for preparing the ZrF_4-based glass fiber in the NTT laboratory. Details are described below. The $ZrF_4(63)$-$BaF_2(33)$-$GdF_3(4)$ system is used for the base glass and AlF_3 is used as a dopant for controlling the refractive index. Starting materials are ZrF_4, BaF_2, GdF_3, and AlF_3 of four-9's purity. The mixture of the starting materials was treated with $NH_4F \cdot HF$ at 400°C for 30 min and melted at 900°C for 2 h in a gold crucible. The glass rod is prepared by pouring the melt into a cylindrical brass mold preheated at about 300°C and then by annealing it for 20 h.

A preform with a core and cladding structure is prepared by a build-in casting method, which was originally developed for preparing fluoride glass fiber. Fig. 10 shows a sequence diagram for the process. The cladding glass melt is cast into the mold, which is preheated at near glass transition temperature and then upset. The melt in the central part in the mold flows out, and the core glass melt is instantly cast into the central hollow part and then annealed. Thus, preform with a core-cladding structure made of fluoride glass in both core and cladding parts can be obtained. In the present process, cladding is carried out in a quasi-liquid phase. Therefore, a smooth core-cladding boundary can be obtained. The preform is jacketed with a Teflon FEP tube, and then, it is zonally heated at 350-400°C by an electric furnace and drawn into the fiber. The fiber is wound on a plastic bobbin. Designed core diameter, ranging from 20 to 80 μm, and outer diameter, ranging from 100 to 300 μm, can be easily achieved. Fiber lengths reach 500 m. The relative refractive index difference between core and cladding could be realized up to 0.5 percent. Fig. 11 shows an interference microscope photograph of a cross section of a fiber with a core diameter of 37 μm, a cladding diameter of 198 μm, and Δn of 0.33 percent.

Drexhage *et al.* reported a crucible technique. The single crucible apparatus used to prepare fluoride glass fibers is depicted in Fig. 12. It consists of a high purity platinum crucible with a lid and a tapered downpipe held within a resistance heated furnace. The crucible is charged with a premelted cullet. Separate thermal control is provided for the nozzle assembly. The design permits the use of inert or reactive (e.g., N_2 or CCl_4) atmosphere above the melt and about the fiber. A cooling fixture is employed to quench the glass as it exits the downpipe orifice. The fiber passes through a coating applicator prior to being wound on a drum. Multimeter lengths of plastic clad fiber are obtained. The working range for fluoride glasses is much narrower than that for silicate glasses in general, i.e., the temperature range for fiber fabrication is limited. This problem is compounded by the high rate of crystallization in the vicinity of 350-400°C. Therefore, fibers must be drawn through the application of a modified single crucible design. HfF_4-BaF_2-LaF_3 and ZrF_4-BaF_2-LaF_3 based fluoride glass fibers have been prepared. Recently, Tran *et al.* succeeded in preparing fibers approaching 1 km in length by a specially

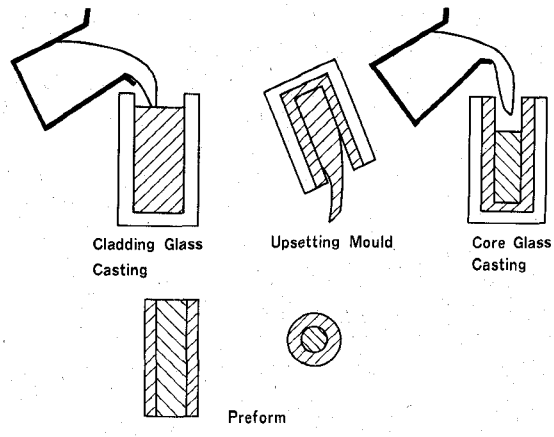

Fig. 10. Schematic of a build-in casting process for a fluoride glass preform.

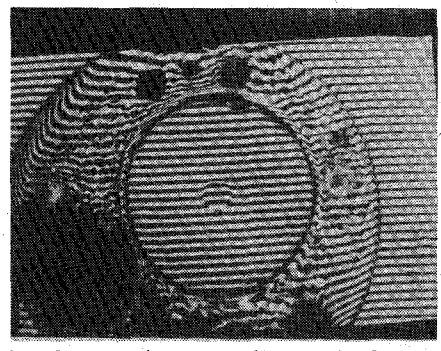

Fig. 11. An interference microscope photograph of a cross section of a fluoride glass fiber with 37 μm core diameter, 198 μm cladding diameter, and Δn of 0.33 percent.

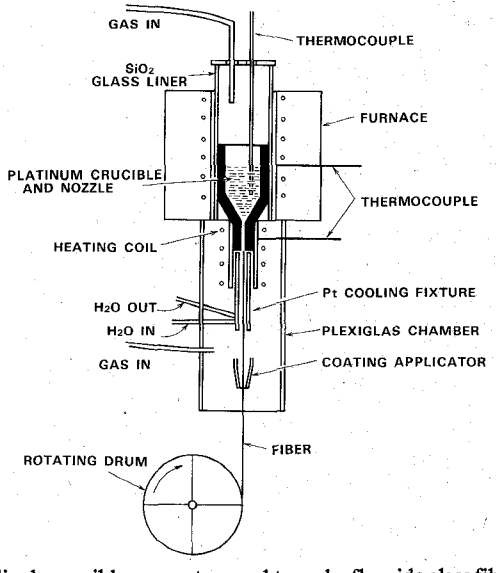

Fig. 12. Single crucible apparatus used to make fluoride glass fibers [32].

designed crucible from a ZrF_4-BaF_2-LaF_3-AlF_3-LiF-PbF_2 glass system having improved viscosity-temperature characteristics [44]. Fiber drawing was carried out by using a two crucible draw setup. Bulk fluoride glasses were preheated to a molten state in a specially designed Pt crucible and were transferred to a gradient free furnace preheated at the glass

softening temperature (about 315°C) for fiber drawing. Alternatively, as shown in Fig. 13, the molten fluoride glasses were drained from an upper melting crucible to a lower single draw crucible maintained at the glass softening temperature range prior to fiber drawing.

B. Chalcogenide Glass Fiber

In general, prior to fiber drawing, bulk materials must be synthesized. Arsenic-sulfide glasses are prepared using six-9's pure arsenic and five-9's sulphur, which is distilled in a reactive S_2Cl_2 gas atmosphere to eliminate water contained in the glass [36]. Reagents to yield 50 g of glass are weighed out into a quartz ampoule with 4 mm thick walls, which is then evacuated and sealed still under a vacuum. The sealed ampoules are heated at 700-900°C for 20-100 h in a rocking furnace to mix the constituents. The ampoules are withdrawn from the furnace to cool naturally in air. Glass rods 8-15 mm in diameter and 80-120 mm in length are obtained.

The obtained glass rod is zonally heated in an inert atmosphere and drawn into a fiber. The problems encountered in fabricating tubes of cladding glass and rod of core glass with optical polished surfaces are severe. Therefore, the preform method is usually limited to fabrication of only unclad fiber.

Kapany and Simms developed the specially designed concentric crucible for drawing arsenic-sulphur glass fibers. Recently, an author and his co-workers succeeded in preparing chalcogenide fiber using a Pyrex glass double crucible assembly, as is shown in Fig. 14. Its design is very similar to the conventional platinum double crucible used for producing silicate fibers, with the exception of a rather long nozzle pipe which is useful for cooling the glass as it exists through the nozzle. This is required due to rather narrow working range in arsenic-sulphur glass.

The crucible is charged with a core glass of $As_{38}S_{62}$ in the inner section and a cladding glass of $As_{35}S_{65}$ in the outer section and is then fitted into the electric furnace. The inside of the furnace is maintained under an inert atmosphere to prevent the formation of arsenic and sulphur oxides. The temperature of the assembly is increased to about 400°C. The core and cladding glasses descend from the nozzle and form a small drawing cone beneath it. The drawing is carried out satisfactorily, if a stable symmetrical cone of flowing glass exists beneath the nozzle. The core to cladding diameter ratio can be varied by changing the nozzle diameter ratio between the inner and outer crucibles. Fibers longer than 1 km are easily fabricated. The fiber diameter ranges from 100 to 300 μm. Fig. 15 shows a clad type arsenic-sulphur fiber wound on a plastic bobbin and Fig. 16 shows a photomicrograph of its cross section.

Bornstein *et al.* have developed a technique of preparing the raw materials and drawing fibers, giving special attention to avoid the forming of oxygen compounds [51].

C. Oxide Glass Fiber

High GeO_2 glass fiber has been fabricated by the VAD process [37]. Germanium tetrachloride ($GeCl_4$) is used as the main raw material and antimony pentachloride ($SbCl_5$) is used as the dopant raw material. $GeCl_4$ and $SbCl_5$ are bubbled with Ar gas and transfered into the oxyhydrogen flame where they are hydrolyzed into oxide particulates, which are deposited on the end of a starting substrate. The substrate is

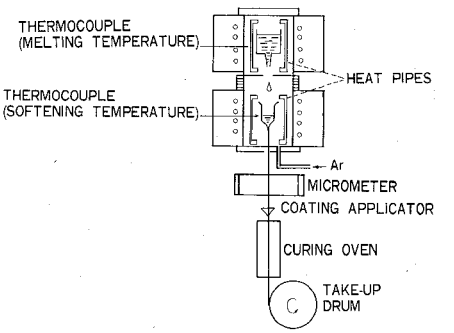

Fig. 13. A two crucible setup used to draw fluoride glass fibers [78].

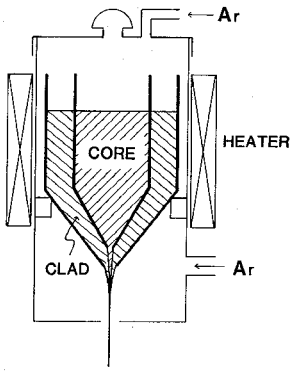

Fig. 14. A Pyrex glass double crucible assembly for preparing arsenic-sulphur glass fibers.

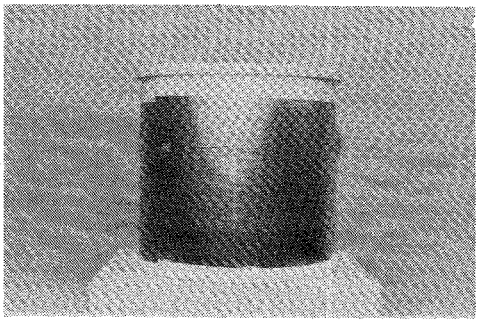

Fig. 15. An arsenic-sulphur glass fiber wound on a bobbin.

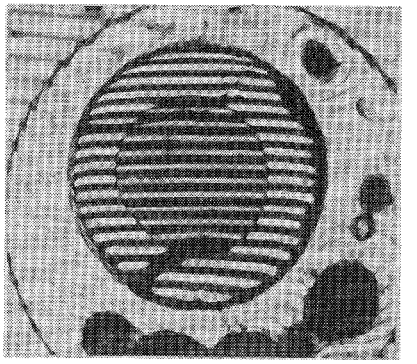

Fig. 16. An interference microscope photograph of a cross section of an arsenic-sulphur glass fiber with 130 μm core diameter, 220 μm cladding diameter, and Δn of 1.0 percent.

spinned and lifted vertically at the constant speed following the oxide deposit growth. A porous preform is sintered to the transparent preform by an electric furnace which is charged with helium gas. The size of the sintered preform is normally 15 mm in diameter and 100 mm in length. The obtained preform is drawn by using the fiber drawing machine which is used for the high silica preform. The furnace temperature is held at about 1000°C. A fiber with 400 m length and 120 μm diameter has been drawn. The fiber was coated with silicone. In the present process, precise control of dopant antimony distribution is not easy due to high volatility of antimony oxide.

A conventional crucible technique can be applied to preparation of various heavy metal oxide glass fibers. Tellurium oxide based glass fibers have been prepared with gold crucibles [54].

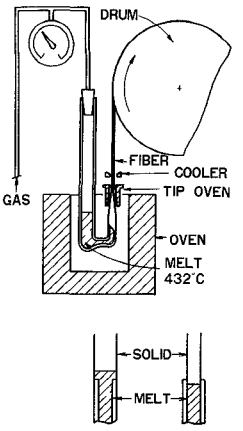

Fig. 17. Schematic of AgBr fiber single crystal growing apparatus [15].

D. Crystalline Fiber

Two approaches have been taken to form crystalline fibers. The first involves solid-state recrystallization by extrusion from the original crystal rod. Using this method, long polycrystalline fibers can be prepared at relatively high speed, although the fiber prepared is generally fragile. The second method consists of growth technique from melt phase, which enables forming single crystal fiber at a rather slow rate.

Polycrystalline fibers without cladding have been extensively made from KRS-5, KRS-6, and TlBr by the extrusion method [7], [16]. The fabrication of KRS-5 fibers is as follows. The starting material is melted in a nitrogen atmosphere, being cast and sealed into glass ampoules. The material is crystallized by the vertical Bridgeman method. The crystal ingot is shaped by mechanical machining to 10 mm in diameter and 30-40 mm in length, ready to be utilized as a fiber preform, which is then extruded into the fiber form through a diamond-wire die built into an apparatus exerting high pressure on a preform in the container. The extrusion temperature is varied from 200 to 350°C, and the extrusion pressure is settled at such a point that a extrusion rate of a few centimeters per minute could be realized. The surface of the KRS-5 fiber thus prepared is observed to be smooth enough, except that it carries a few scratches 1-2 μm in width. AgCl can also be easily extruded into fiber.

EFG (edge-defined film-fed growth) technique or a modification of this technique is used for materials that are difficult or impossible to extrude or that do not form glasses. Single crystal optical fibers have been grown from AgBr, CsI, and so on. Bridges *et al.* reported the growth experiment with AgBr [15]. Fig. 17 shows a schematic of fiber crystal growing apparatus. The liquid charge is contained in a fused-quartz *U* tube, which is kept molten by a surrounding oven. Fiber growth occurs close to the exit of a nozzle, which terminates one arm of the *U* tube. The rate of liquid fed to the nozzle can be sensitively controlled by N_2 gas pressure applied to the other arm of the *U* tube. A small oven around the nozzle tip with independently adjustable temperature and a water cooled element adjustable in position enable the interface to be accurately positioned. Smooth clear fibers with diameters between 0.35 and 0.75 mm have been grown at rates up to 2 cm/min. Stable crystal growth is indicated with the (100) direction along the fiber axis. Crystalline imperfections, which appear under insufficiently stable growth conditions, appear to be low-angle dislocations or grain boundaries.

CsI fiber have been grown from the melt utilizing the modified pulling down method [59]. Crystalline fibers with diameters between 0.7 and 1.0 mm, and lengths up to 1.5 m have been grown at rates between 5 and 6 mm/min.

In addition, filaments of alkali halides such as LiF, NaCl, and CaF_2 are grown from the melt. However, their optical properties have not yet been reported [6].

IV. Optical Properties

Spectral loss and dispersion are two fundamental characteristics for infrared fibers, similarly for silica glass fibers. In this section, techniques for measuring these characteristics are described first and then spectral loss and dispersion for various infrared fibers are summarized.

A. Measurement Techniques

Loss measurements for infrared fiber have been carried out in the spectral range from visible to mid-infrared wavelength by using monochromators or lasers. Refractive index spectra have been measured for several bulk materials and dispersion characteristics have been numerically estimated from their measured data. The characterization techniques for infrared fibers are the same in principle as for silica fibers, except optical devices operating in the wavelength of interest should be used.

1) Spectral Loss: Spectral loss for infrared fibers is measured in the wide wavelength range from 0.7 to 11 μm [61]. The 0.7-1.8 μm band can be covered with the conventional test set developed for the silica fiber. In the wavelength range from 1.8 to 11 μm, the optoelectronics system was specially designed, which is shown in Fig. 18. This system is composed of a platinum resistance heater as a light source, a stepscanning monochromator, an InSb detector or an HgCdTe detector cooled with liquid N_2, a current-sensitive preamplifier, a lock-in amplifier, a digital voltmeter, a minicomputer, and a hard copy unit. The platinum lamp with 100 W power generates high output power in the infrared wavelength. The monochromatic light, with about 50 Å half power linewidth, is obtained by the monochromator with gratings blazed for 3.5 and 7.5 μm.

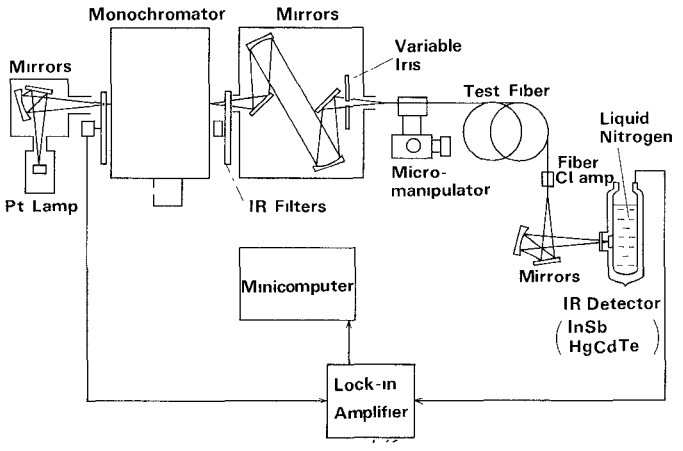

Fig. 18. Spectral loss measurement system for infrared fibers.

In order to eliminate the second-order spectrum in the output spectrum from the grating monochromator, four kinds of infrared bandpass filters with cutoff wavelengths of 1.8, 2.5, 4.3, and 7.6 μm are used. They are inserted automatically into the optical system. The optical system is composed of infrared mirrors. The numerical aperture in the light injection can be varied in the range from 0.01 to 0.2.

The fiber output signals are detected with InSb in the 1.8-5.5 μm and with HgCdTe in the 5-11 μm wavelength regions. Maximum detectivity (D^*) is 1.4×10^{11} cm · Hz/W at 10.6 μm for the HgCdTe detector. Both detectors have 2 mm diameter active areas. The detected optical signal is amplified by the current-sensitive preamplifier with an amplification factor of 50 dB and fed into the lock-in amplifier. The amplified signals are measured with a signal voltmeter with IEEE 488 compatible interface. Then, they are stored in a minicomputer (Tektronix 4051). In the present system, data correcting, data processing, and graphic display are carried out by the minicomputer. Measured results are obtained from a hard-copy unit.

Table VII shows specifications for the present spectral loss measuring set. The dynamic range for the present system is about 25 dB in the 2-10 μm wavelength region. The error is estimated to be smaller than ±0.05 dB/km for a 50 m long fiber with 20 dB/km. In addition to spectral loss, transmission losses are measured at several specific wavelengths by using various lasers such as HF, DF, CO, and CO_2 lasers. The transmission loss measurement is usually carried out by the conventional cut-back method.

2) Spectral Refractive Index: The refractive index is measured on a triangular shaped bulk prism by the minimum deviation method. A precision spectrometer (Kalnew GMR-1S) is used to determine the spectral refractive index in the NTT laboratory [23]. It covers the wavelength range from 0.4 to 4.26 μm, in which refractive index behavior is significant for almost all infrared materials. Refractive indexes are measured at 42 wavelengths. Mercury, helium, and hydrogen emission lines are used for wavelengths up to 2.5 μm. Beyond 2 μm, a platinum wire heater is used and the measuring wavelengths are identified by the absorption bands of 1.2.4-trichlorobenzene and polystyrene.

A photomultiplier with high sensitivity is used as a detector

TABLE VII
SPECIFICATION OF SPECTRAL LOSS MEASURING SET FOR INFRARED FIBERS

Wavelength range (μm)	0.7 - 11
Wavelength interval (μm)	0.01
Linewidth (μm)	0.005
Dynamic range (dB)	25
Numerical aperture	0.01 - 0.2
Accuracy (dB/km)	0.01 (20 dB/km X 50 m fiber)

for the emission line spectra in the wavelength range of 0.4-0.8 μm and an indium antimonide detector operated at liquid nitrogen temperature for the longer wavelengths. In both cases, the incident light flux is chopped at 270 Hz and the detected optical signal is amplified by a low-noise current sensitive preamplifier. The amplified output signal is fed into a lock-in amplifier and the lock-in amplifier output signal is recorded as a function of the minimum-deviation angles for each line. All measurements are made at 23 ± 1.0°C. Measurement error in the present apparatus is within 0.0001.

The measured refractive indexes are fitted to the conventional dispersion of the following form:

$$n(\lambda) = \frac{A}{\lambda^4} + \frac{B}{\lambda^2} + C + D\lambda^2 + E\lambda^4 \tag{2}$$

where λ is the wavelength and coefficients A-E are constant. Material dispersion $M(\lambda)$ can be obtained as

$$M(\lambda) = \frac{\lambda}{c} \cdot \frac{d^2 n(\lambda)}{d\lambda^2} = \frac{2}{c}\left(\frac{10A}{\lambda^5} + \frac{3B}{\lambda^3} + D\lambda + 6E\lambda^3\right). \tag{3}$$

B. Loss Characteristics

Spectral losses have been measured for fluoride glass fibers in the wavelength range from 0.7 to 4.2 μm, for chalcogenide fibers in the 0.7-11 μm, for heavy metal oxide glass fibers in the 0.7-12 μm, and for halide crystal fibers in the 0.6-11 μm, including several laser wavelengths.

1) Fluoride Glass Fiber: Transmission loss spectra have been obtained for two kinds of fibers. The first is plastic clad fiber—fluoride glass core-Teflon FEP cladding. The second is clad type fiber—fluoride glass core-fluoride glass cladding. Fig. 18 shows a transmission loss spectrum for a Teflon FEP clad fiber, which is drawn from an AlF_3 doped ZrF_4-based glass rod cladded with a Teflon FEP tube [62]. The core diameter is 200 μm and the outer diameter is 300 μm, and refractive indexes of core and cladding are 1.517 and 1.338, respectively. Transmission loss decreases with increasing wavelength in the shorter wavelength region and increases steeply with wavelength in the longer wavelength range. The former is due to metal impurities, which will be described in detail in the following. The latter arises dominantly from the infrared vibrational absorption of the glass. Several of the peaks appear in the measured wavelength region. The large peak centered at 2.9 μm is caused by the fundamental stretching vibration of OH ions. The small hump at 4.1 μm originates from the Teflon FEP cladding. Minimum transmission losses are 88 dB/km at 2.6 μm and 470 dB/km at 3.5 μm.

Fig. 20 shows a loss spectrum for a fluoride glass clad type fiber [30]. The core diameter $2a$ is 37 μm and the cladding

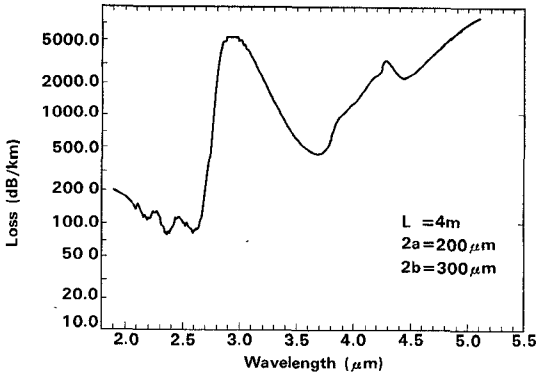

Fig. 19. Spectral loss for a fluoride glass core-Teflon FEP cladding fiber.

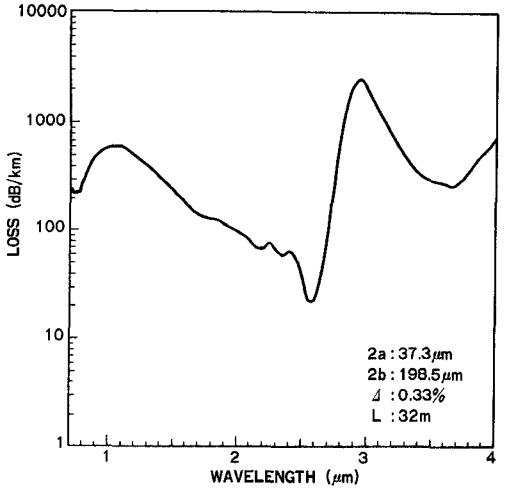

Fig. 20. Spectral loss for a fluoride glass core-fluoride glass cladding fiber.

diameter is 198 μm. Then the cladding-core diameter ratio is 5.26. The refractive index difference between core n_1 and cladding n_2 is 0.33 percent (numerical aperture = 0.123), which is almost constant in the 0.546-4 μm wavelength region. Normalized frequency V at the wavelength of operation λ is given as follows:

$$V = \frac{2\pi a}{\lambda}\sqrt{n_1^2 - n_2^2}. \quad (4)$$

In the present fiber, V value is 5.6 at 2.55 μm, at which the minimum loss is obtained as mentioned below. The fundamental to the fifth modes could be transmitted at 2.55 μm. Beyond $\lambda = 5.9$ μm, V becomes less than 2.405 and single mode condition is satisfied. Single mode operation would be achieved at $\lambda = 2.55$ μm, if the core diameter was smaller than 15.8 μm in case of 0.3 percent refractive index difference between core and cladding.

A smooth core-cladding boundary, which is formed by the build-in casting technique, leads to a remarkable reduction of optical loss. The feature of spectral loss of the present fiber is very similar to that for the Teflon FEP clad fiber. However, the small hump centered at 4.3 μm, which is observed in the latter, disappears in the former. This is due to the fact that the transmitted power is sufficiently confined to the core in the fiber cladded with fluoride glass. The huge attenuation in a shorter wavelength range of less than 2.5 μm is caused by impurity metal ions. Spectral absorptions of $3d$ transition metal ions and rare earth ions are quantitatively measured in ZrF_4-based glass [25], [26]. The $3d$ transition elements such as Fe, Cu, Cr, etc., have their absorption peaks in the near infrared wavelength region shorter than 2.5 μm. On the other hand, some of the rare earth ions show large absorptions beyond the 2.5 μm region. Based on these data, the fiber loss spectrum can be analyzed and the result indicates that Fe^{2+} and Cu^{2+} are the dominant obstacles, which contaminate the glass with 1 ppm level or less. It was also clarified that impurity concentration in fluoride glass fibers should be reduced to a 1 ppb level or less in order to attain an ultralow loss value.

The small peaks at 2.25 and 2.45 μm are due to combined overtones between the OH stretching vibration and glass matrix vibration of Zr-F and Ba-F bonds, respectively. The minimum loss is 21 dB/km at 2.55 μm, which is three orders of magnitude smaller than the loss at the same wavelength in high silica fiber.

Optical transparency of numerous ZrF_4-based glasses other than the ZrF_4-BaF_2-GdF_3 system has been examined spectroscopically. For example, Lucas has measured optical transmission for bulk glass in a system with a composition giving a candidate for fiber processing [63]: ZrF_4(57)-BaF_2(34)-LaF_3(5)-AlF_3(4). Examination of UV and IR edges indicates the optical window lies from 0.2-0.3 to 6-7 μm.

HfF_4-based glasses have also been tested optically in which the multiphonon absorption edge locates in the longer wavelength side with respect to the ZrF_4-based materials mentioned above [24]. A series of fluoride glasses which do not contain hafnium or zirconium such as ThF_4-based rare earth based and combined BaF_2-ZnF_2 glasses exhibit enhanced infrared transmission extending from 0.25 μm to 9-10 μm [24]. However, their optical losses have not yet been measured for drawn fibers.

$ZnCl_2$ is suggested to be a potentially useful material for ultralow loss fibers in the 3.5-4 μm wavelength region, based on the numerical estimation of scattering and lattice absorption losses [5]. However, its optical fiber characteristics have not been reported.

2) Chalcogenide Glass Fiber: Kapany and Simms [1] obtained spectral transmission data on As-S fiber in 1965, which showed relatively high loss. Recently, the authors measured spectral losses for an unclad fiber drawn from an As-S glass rod [36], and for a clad type fiber drawn by the double crucible technique [49]. Fig. 21 shows the spectral loss for the unclad arsenic-sulphide glass fiber. Transmission loss decreases with wavelength in the shorter wavelength region. This part in the curve corresponds to a tail of the fundamental absorption edge, which may in fact be related to some defects and impurities in the glass. It is worthwhile to note that the absorption tail in the present fiber is considerably lower than the one presented by Wood and Tauc [77]. This enabled us to obtain low loss in the 2 μm band. Several of the peaks which appear in the measured wavelength region are caused by hydrogen impurities in the material. The peak at 2.92 arises from the fundamental stretching vibration of the OH ion combined to arsenic. The small peak at 1.43 μm is assigned to the second

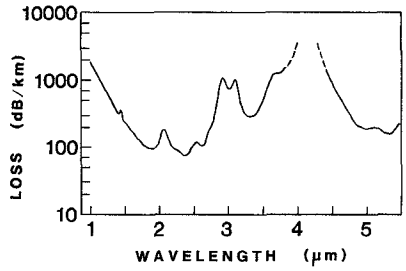

Fig. 21. Spectral loss for an unclad arsenic-sulfide glass fiber: 200 μm diameter.

overtone of the fundamental OH vibration. A small hump observed from 2.28 μm is the result of the combinational vibration between the fundamental OH ion vibration and the As-S bond vibration. This peak height is observed to be proportional to absorption intensities for the fundamental OH ion vibration around 3.0 μm for the various arsenic-sulphide fibers.

The more pronounced peak centered at 4.09 μm is due to SH ions, contaminating the material during the preparation process. The peak at 2.08 can be assigned to overtones of the fundamental vibration of the SH ion at 4.09 μm and the peaks at 2.54 and 3.11 μm originate from the combinatorial vibration between the SH ion and the glass matrix As-S bond vibrations, respectively. These are in fact hardly observed for a low SH content fiber. Although the curve is not shown in Fig. 21, it is confirmed that the optical loss shows a rapid increase with wavelength in a wavelength region longer than 6.0 μm. This arises from multiphonon absorption in the glass matrix.

As is shown in Fig. 21, the lowest loss of 78 dB/km at 2.40 μm is obtained and the minimum losses of 92 dB/km at 1.85 μm, 295 dB/km at 3.30 μm, and 164 dB/km at 5.30 μm are observed. The loss at the CO laser wavelength of 5.25 μm is 170 dB/km, which may be the result of slight contamination by an oxide impurity.

The spectral loss for the clad type arsenic-sulphur glass fiber exhibits almost the same characteristics as that for unclad fiber, as mentioned above.

For an As_2Se_3 core-As_2S_3 cladding fiber, the losses of 10 dB/m in the spectral range of 4.5–6 μm are obtained, while the predicted minimum losses in these glasses are close to 0.05 dB/km in the spectral region 4–5 μm [35]. A CO_2 laser transmission measurement was carried out on the As_2Se_3 fiber, which was drawn from oxygen-free raw material inside an Ar atmosphere glove box [51]. Preliminary attenuation measurements indicate that the attenuation is better than 0.1 dB/cm.

Fig. 22 shows a loss spectrum for GeS_3 unclad fiber which is drawn from a glass rod [52], which is subjected to OH, SH reduction treatment. Strong absorption peaks at about 3, 4, and 5 μm wavelengths originate from OH, SH, and C impurities, respectively. The GeS_3 glass fiber shows four optical windows with losses lower than 1 dB/m: 0.36 dB/m at 2.4 μm, 0.85 dB/m at 3.3 μm, 0.56 dB/m at 4.7 μm, and 1 dB/m at 5.1 μm. The lowest optical loss for GeS_3 is at 2.4 μm. $Ge_3PS_{7.5}$ unclad fiber is also drawn and shows a spectral loss similar to that for GeS_3 fiber [34].

Fig. 23 shows spectral loss for an unclad arsenic triselenide

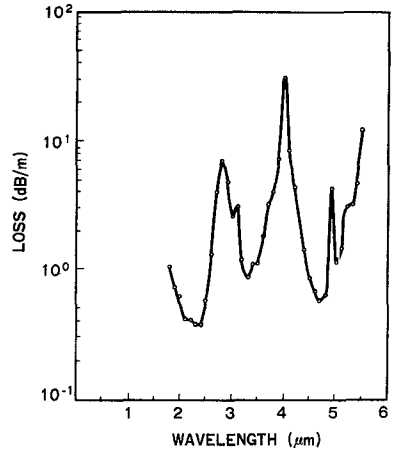

Fig. 22. Spectral loss for a GeS_3 glass unclad fiber: 200 μm diameter.

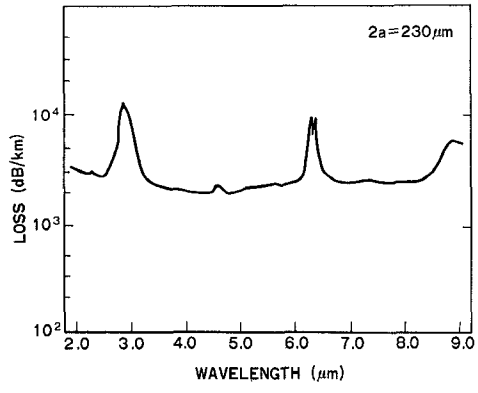

Fig. 23. Spectral loss for an As_2Se_3 glass unclad fiber: 200 μm diameter.

glass fiber [49]. It has relatively high and flattish losses in the wavelength range measured. Loss spectrum is also obtained in the 3–11 μm wavelength range for unclad $As_{15}Ge_{30}Se_{55}$ glass fibers, which are drawn from rods synthesized in sealed silica ampoules at 1000°C. They have losses of 10 dB/m in the wavelength range from 5.5 to 7 μm and 20 dB/m from 8.5 to 10.6 μm [54].

La-Ga-Ge-Se glass is well known to be highly transparent in a wide band [55]. However, fiber drawing has not been reported yet.

3) Oxide Glass Fiber: Fig. 24 shows the loss spectrum for a germanate glass fiber with Sb_2O_3-doped GeO_2 core and GeO_2 cladding [64]. Several absorption peaks due to silicone resin coating and OH ions are observed, and the attenuation loss decreases with increasing wavelength in the shorter wavelength region. A minimum loss as low as 13 dB/km has been achieved at 2.05 μm and the second minimum loss is 70 dB/km at 2.4 μm. It is suggested that the attenuation in the longer wavelength region beyond 2.1 μm up to 2.6 μm would be considerably reduced if germanate glass cladding with sufficient thickness were provided and an excellent dehydration technique were introduced into the preform fabrication process.

The analytical research indicates that an attenuation less than 0.1 dB/km could be achieved in a practical sense around 2.2–2.4 μm wavelength [39]. Another estimation of UV and IR absorptions as well as Rayleigh scattering showed that the

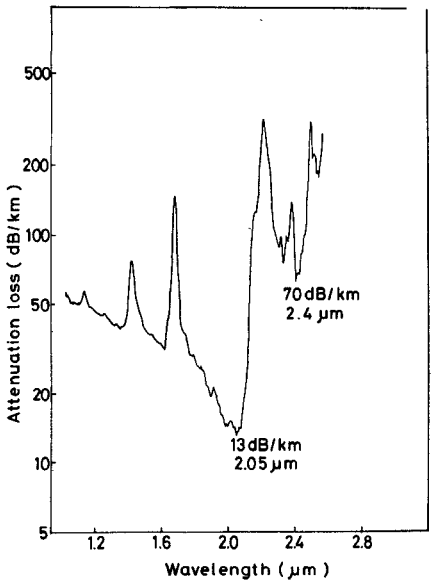

Fig. 24. Spectral loss for a germanium oxide glass fiber: Sb_2O_3-doped GeO_2 core; GeO_2 cladding.

predicted minimum loss in GeO_2 glass is close to 0.25 dB/km at 2 μm [35]. This discrepancy should be clarified in the course of fabrication of practical low loss fiber.

The loss spectrum for 200 μm diameter TeO_2-based glass fiber [54], which is made from dehydrated glass by using a conventional drawing apparatus at 400°C, is obtained. It shows relatively high losses of 1 dB/m at 2 μm and 20 dB/m at 4 μm.

4) Halide Crystal Fiber: The theoretical analysis shows that a minimum intrinsic attenuation in the projected curve is extremely low for crystalline fibers among various IR fibers. The obtained losses in practical crystalline fibers, however, are substantially greater than those projected.

Among many crystalline fibers, polycrystalline KRS-5 fibers have been the most extensively investigated. The optical transparency of these fibers covers a much broader spectral range and extends from approximately 0.6 μm in the visible to 35 μm in the IR. Bulk loss measurements are made by the standard calorimetric techniques and fiber attenuation has generally been measured by using CO, CO_2, HF, and DF laser sources.

In general, optical loss decreases monotonically with increasing wavelength. This is a result of decreased scattering loss with wavelength, which might be due to the existence of micro grains. The reported transmission loss at 10.6 μm ranges from less than 0.4 dB/m to 0.7 dB/m, in which the lowest loss of 0.35 dB/m is obtained for the best quality fiber [13]. Loss at 5 μm is twice that at 10.6 μm. The nature of fiber loss has been determined by measuring the scattering loss [65]. The experiment indicates that scattering loss and absorptive loss are approximately equal at 10.6 μm. The effects of fiber grain size and bending radius on transmission loss have also been studied [14]. It is found that polycrystalline KRS-5 fiber is frail against bending. Transmission losses for polycrystalline AgCl and AgBr fibers were measured in 2.5–25 μm. The minimum loss of 0.06 dB/cm was obtained at 14 μm for the former fiber [10]. Similar transmission results were obtained on AgBr fibers, although the transmission window for the latter extends to longer wavelength up to 25 μm than that for the former.

The ultimate low losses for single crystal fibers grown from TlCl, TlBr, KRS-5, KRS-6, AgCl, KBr, and KCl are evaluated to be 10^{-3}–10^{-5} dB/km. However, the materials for which fiber loss measurement have been carried out are limited to a small number of crystals.

The experiment on AgBr single crystal fiber indicates a loss of about 2×10^{-2} cm^{-1} at 10.6 μm, which appears to be due to impurity absorption [15]. The ultimate loss of pure AgBr would be estimated to be 10^{-3} dB/km range around 5 μm [15].

Transmission loss measurements are also carried out for CsI and CsBr single crystal fibers [59]. The losses for 0.7 mm diameter and 1.5 m long CsI fiber with a Teflon FEP loose cladding and that for CsBr fiber are 80 and 5 dB/m, respectively. It requires material purification and a great improvement in the fabrication process to reduce optical loss further in both poly- and single-crystal fibers.

C. Dispersion Characteristics

The dispersion is a very important parameter, which is related to the transmission bandwidth of the fiber.

To date, however, dispersion characteristics have not been measured on practical infrared fibers and only numerical evaluations of the material dispersion have been carried out based on the measured spectral refractive index in several infrared materials.

1) Fluoride Glass Fibers: Material dispersion in fluoride glass has been most extensively investigated among infrared materials for optical fibers. It was clarified that zero-material dispersion wavelengths are located at the 1.4–1.8 μm band and the slope of the dispersion versus wavelength is gentle compared with that for high silica fiber [22], [23].

Fig. 25 shows the refractive index spectra for ZrF_4-BaF_2-GdF_3 and AlF_3-BaF_2-CaF_3-YF_3 glasses. The curves are remarkably smooth and the fit between the measured point and the curve is excellent because of the high measurement accuracy and the high optical quality in the tested fluoride glasses. The computed coefficients A–E in (2) for the glasses are shown in Table VIII. Material dispersion $M(\lambda)$ can be obtained using (3). The computed material dispersion spectra are given in Fig. 26. The zero-material dispersion wavelength is 1.62 μm for ZrF_4-BaF_2-GdF_3 glass and 1.48 μm for AlF_3-BaF_2-CaF_2-YF_3 glass, as listed in Table VIII. It is noted that zero material dispersion wavelengths are somewhat shorter than the predicted minimum-loss wavelengths. Fortunately, however, the slopes of the dispersion curves are gentle, as their refractive indexes change gently with wavelengths. Material dispersions at the projected minimum loss wavelengths are 3.2 ps/Å · km at 3.4 μm for the ZrF_4-based glass and 2.5 ps/Å · km at 2.7 μm for the AlF_3-based glass.

Fig. 27 shows refractive index spectra for AlF_3-doped ZrF_4-based glasses in the 0.7–4 μm wavelength region. It is noted that the 0.33 percent refractive index difference between 2 mol% AlF_3-doped glass and 6 mol% AlF_3-doped glass is almost constant in the wavelength region measured. For other ZrF_4-based glasses such as ZrF_4-BaF_2-LaF_3 and HfF_4-based

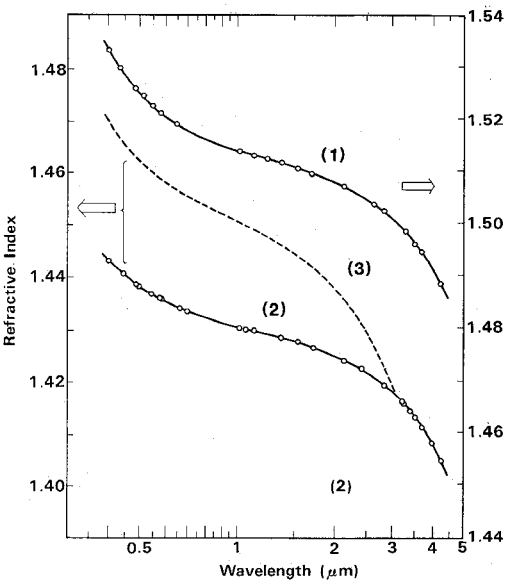

Fig. 25. Refractive index spectra for ZrF_4-based glasses.
(1) $ZrF_4(63)$-$BaF_2(33)$-$GdF_3(4)$.
(2) $AlF_3(40)$-$BaF_2(22)$-$CaF_2(22)$-$YF_3(16)$.
(3) SiO_2.

TABLE VIII
DISPERSION CHARACTERISTICS OF FLUORIDE GLASSES

Composition	Coefficients in eqn.2					
	A x 10^6	B x 10^3	C	D x 10^3	E x 10^6	λ_o^*
$ZrF_4(63)$-$BaF_2(33)$-$GdF_3(4)$	93.6707	2.94329	1.51236	-1.25045	-4.01026	1.62
$AlF_3(40)$-$BaF_2(20)$-$CaF_2(20)$-$YF_3(20)$	7.67742	2.16195	1.42969	-1.28304	-5.35487	1.48

* Zero-material dispersion wavelength(μm)

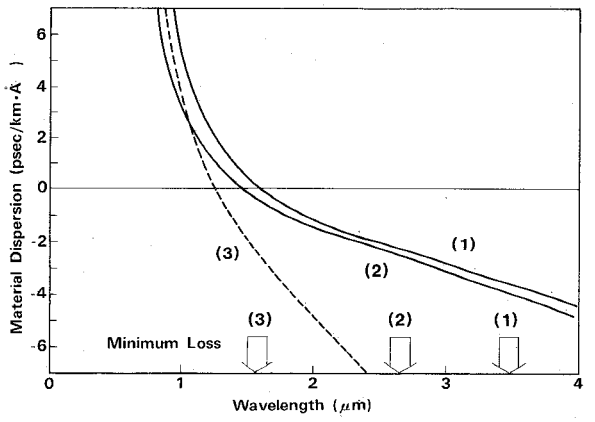

Fig. 26. Material dispersion spectra for fluoride glasses compared with that for pure silica glass. (1) $ZrF_4(63)$-$BaF_2(33)$-$GdF_3(4)$. (2) $AlF_3(40)$-$BaF_2(22)$-$CaF_2(22)$-$YF_3(16)$. (3) SiO_2.

glasses, several studies have also been carried out on refractive index and material dispersion [22], [66]. The examinations indicate that the zero-material dispersion wavelengths are in the vicinity of 1.6–1.7 μm for both glasses and the dispersion curve is considerably flatter. The trends are very similar to that for ZrF_4-BaF_2-GdF_3 glass described above. The feature holds true in glasses containing additional components. These results compare favorably with theoretical predictions by Nassau [21].

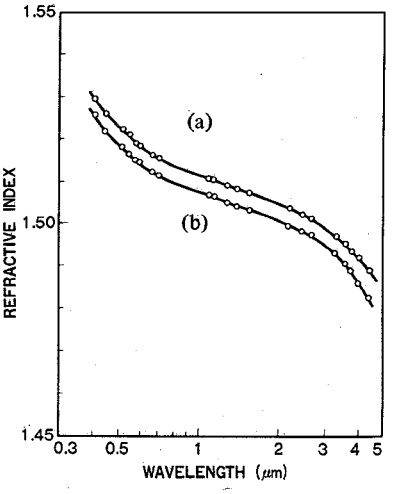

Fig. 27. Refractive index spectra for AlF_3-doped ZrF_4-based glasses. (a) 2 mol% AlF_3-doped glass. (b) 6 mol% AlF_3-doped glass.

In addition to material dispersion, taking into consideration waveguide dispersion, which compensates material dispersion, the range of choice in Δn and core diameter available to give zero total dispersion at particular wavelengths was discussed by Gannon [55]. For example, the optimum core size would appear to be around 12 μm, which would give zero total dispersion at a wavelength of 2.5 μm. At the lower loss wavelength of 3 μm, a total dispersion of about 3 ps/Å · km would be estimated. This would allow a system bandwidth of beyond 300 GHz/Å · km. Thus, fluoride glasses offer the potential for very large information carrying bandwidths over a wide spectral range.

2) Chalcogenide Glass Fiber: The refractive index of arsenic trisulfide glass was measured and constants for the dispersion equation were given by Malitson *et al.* [16]. Material dispersion calculated from the data is shown in Fig. 28. Material dispersion of As_2S_3 glass falls to zero at 4.89 μm, which coincides fortunately with the predicted loss minimum wavelength. It is also noted that the slope of the curve is relatively lower, compared with oxide or fluoride glasses. The refractive index spectrum of GeS_3 glass was also obtained in the wavelength range from 0.5 to 3.5 μm [68].

3) Oxide Glass Fiber: The refractive index spectrum of GeO_2 glass has been measured in the optical range 0.5–2.5 μm. From the result of the measurement, material dispersion is calculated and zero dispersion wavelength is estimated to be 1.69 μm [39]. For other oxide glasses for infrared fiber, few refractive index spectra have been reported.

4) Halide Crystalline Fiber: Refractive indexes for several halide crystals in infrared fiber have been available in pertinent literature. From these data, dispersion characteristics could be discussed. Recently, however, based on the optical oscillator strengths and excitation energies [69], the zero material dispersion wavelength is identified for a wide range of oxides, fluorides, chlorides, and bromides by Nassau [70], including halide crystals for infrared fibers. Theoretically calculated zero material dispersion wavelengths for typical halide fiber materials are given in [21]. They are located in a considerably longer wavelength side than those for oxide, fluoride, and chalcogenide glasses. This might be related to the fact that halide

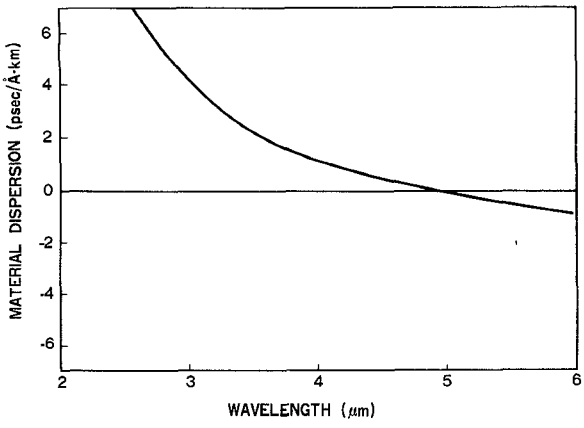

Fig. 28. Material dispersion curve for As_2S_3 glass.

crystals transmit in a broader wavelength range than the other materials. The material dispersion slope at zero dispersion wavelength is also calculated. The result indicates that halide crystals such as KRS-5 and CsI show much smaller slopes than oxide, chalcogenide, and fluoride glasses.

V. Applications

Applications of infrared fibers can be classified into the following two fields: long distance communication and short length application.

Infrared fiber has a potential ultralow loss of 0.01 dB/km or less in the mid-infrared wavelength range from 2 to 6 μm, as mentioned above. The achievement of such ultralow loss fibers would find applications in very long repeaterless communication links. Transmission in the infrared region would exhibit great merits of not only ultralow loss but also large tolerance at splices and low dispersion, as described above. Recently, Jeunhomme discussed single mode fiber design for the 4 μm band, taking into consideration the splicing and cabling added losses and showed that added losses as small as 0.01 dB/km could be obtained with suitable fiber design and careful handling [71].

The lowest loss achieved to date in infrared fiber is 21 dB/km, which is higher by four orders of magnitude or more than that predicted. In order to reduce transmission loss further and reach the intrinsic material-limited loss, great improvements should be made in both the fabrication process and material.

The second type of application of infrared fibers is a short length application: delivery of high powers such as for laser surgery and machining, and remote infrared sensors such as temperature, thermal images, and radiation. For these applications, low loss is desired, but losses as high as 0.3 dB/m are tolerable, and dispersion chararcteristics are not important. However, mechanical properties as well as power handling capability are matters of great concern.

Among infrared fibers developed polycrystalline KRS-5 fiber has most extensively been used as the flexible lightguide for CO_2 laser power. Tensile strength and power transmission capability were tested for KRS-5 fibers [13], [14]. The 250 μm diameter fiber with an average grain size of 4 μm shows the average yield strength of 5800 psi and the average ultimate strength of 9200 psi, respectively, under the test conditions of 0.02 cm/min crosshead speed and 10 cm gauge length. It was found that the tensile strength is strongly dependent on the fiber grain size and, in general, the smaller the grain size, the greater the strength.

Power transmission capability has also been measured by several researchers [13], [14]. It has been experimentally demonstrated that a CW laser output power of 68 W is transmitted by a KRS-5 fiber with 1 mm in diameter and 0.87 m in length. Transmission as a function of bend radius and cyclic flexure has also been measured [14]. The test shows that transmission remains constant until a bend radius reaches 3.5 cm for 500 μm, or 2.0 cm for 250 μm diameter fibers. It was also demonstrated that transmission over a 1.0 mm diameter fiber remains almost unchanged under 50 000 times cyclic deformation of the minimum bend radius of 20 cm. It should be pointed out that a small radius bend may cause a permanent deformation in fiber because of the large ductility of KRS-5 and may cause a degradation in optical transmission. Therefore, the fiber should be cabled to minimize bending deformation of the fiber.

At the CO_2 laser wavelength, the absorption coefficient for biological tissues is greater than 1000 cm^{-1} and the scattering coefficient is essentially zero [75]. Therefore, the CO_2 laser has clear advantages for use in laser surgery to produce well-controlled incisions. The flexible cable for CO_2 laser surgical use is being developed using KRS-5 fiber [13]. It is designed to deliver 20 W of CW CO_2 laser and to bend down to 20 cm of radius in any direction.

Infrared fiber could be applicable to a laser machining system, especially laser machining equipment with relatively lower power. Machining of plastic, wood, and cloth has been tried by using KRS-5 fiber cable as a light guide of CO_2 laser. The output end of the fiber is easily mounted on the end of a marker pen of the conventional X-Y plotter.

For ZrF_4-based glass fibers, the 2.7 μm-band power delivery characteristics have been investigated using an HF laser emitting at 2.6-3.0 μm wavelengths [72]. Fig. 29 shows a layout diagram for the energy transmission experiment. The fiber consists of a 300 μm fluoride glass core and a 400 μm Teflon FEP cladding. Typical delivered power, without fiber damage, exceeds 0.6 W for a 4 m long fiber, corresponding to a transmission efficiency of about 30 percent. The power transmission capability in the 2.7 μm band makes the fluoride glass fiber attractive as a flexible lightguide for laser printers and other applications such as electronic parts machining.

Infrared fiber can also be applicable to remote monitoring of temperature, infrared image, and radiation. Fig. 30 shows the blackbody radiation maximum wavelength versus temperature, given by Wien's displacement law. As is shown in this figure, radiation at the 10.6 μm band gives rise to a good means of sensing relatively low temperature around room temperature. Infrared fiber will be used for temperature monitoring of unaccessible bodies. Infrared fibers could also be adoptable for a receiver detecting CO_2 laser radiation [14]. The transmission characteristics of laser pulses through KRS-5 fiber demonstrates that the fibers may be used to form the basis of an infrared fiber early warning receiver on an aircraft.

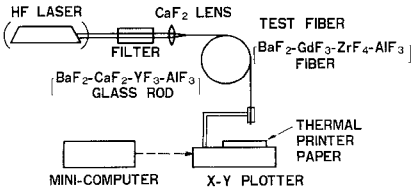

Fig. 29. Layout diagram for laser printer system using a fluoride glass fiber as a power guide.

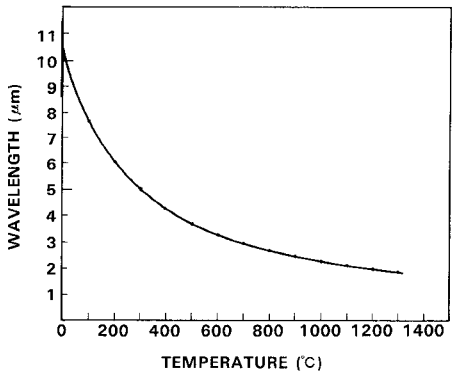

Fig. 30. Radiation maximum wavelength versus temperature in black body.

Infrared fiber will find increasing applications in a variety of fields. These applications, however, require material and process developments.

VI. Conclusion

This paper describes the present state of the art review on infrared fibers. Investigations on the theoretical and experimental problems associated with the selection and evalution of materials suitable for infrared fiber have been carried out. The basic technology of fiber fabrication has also been developed. As a consequence of extensive investigations, various glass and crystalline fibers have been developed which are capable of transmitting infrared wavelength light and fundamental properties have been examined. Thus, infrared fibers have passed through the initial barrier in the course of their development. Infrared fiber technology is a growing field of great interest and, in the future, it will show remarkable progress. Further investigations will be directed toward the development of the respective fibers suitable for various application fields.

Acknowledgment

The authors would like to thank Dr. Giallorenzi for inviting them to present this review.

References

[1] N. S. Kapany and R. J. Simms, "Recent developments of infrared fiber optics," *Infrared Phys.*, vol. 5, pp. 69–80, 1965; also in N. S. Kapany, *Fiber Optics, Principles and Applications.* New York: Academic, 1967.

[2] F. P. Kapron, D. B. Keck, and R. D. Maurer, "Radiation losses in glass optical waveguides," *Appl. Phys. Lett.*, vol. 17, pp. 423–425, 1970.

[3] T. Miya, Y. Terunuma, T. Hosaka, and T. Miyashita, "Ultimate low-loss single-mode fibre at 1.55 μm," *Electron. Lett.*, vol. 15, pp. 106–108, Feb. 1979.

[4] D. A. Pinnow, A. L. Gentile, A. G. Standlee, and A. Timper, "Polycrystalline fiber optical waveguide," *Appl. Phys. Lett.*, vol. 33, pp. 28–29, July 1978; also in D. A. Pinnow *et al.* in *Tech. Dig. CLEA*, 1977, post deadline paper.

[5] L. G. Van Uitert and S. H. Wemple, "$ZnCl_2$ glass: A potential ultralow-loss optical fiber material," *Appl. Phys. Lett.*, vol. 33, pp. 57–59, July 1978.

[6] C.H.L. Goodman, "Devices and materials for 4 μm band fiber optical communication," Joint Spec. Issue, *IEEE J. Solid-State Circuits and IEEE Trans. Electron Devices*, Sept. 1978.

[7] A. L. Gentile, M. Braunstein, D. A. Pinnow, J. A. Harrington, L. M. Hobrock, J. Mayer, R. C. Pastor, and R. R. Turk, "Infrared fiber optical materials," in *Fiber Optics*, B. Bendow and S. S. Mitra, Eds. New York: Plenum, 1979, pp. 105–118.

[8] J. A. Harrington, "Infrared fiber optics for CO_2 laser applications," in *CO_2 Laser Devices and Applications, Proc. SPIE*, vol. 227, pp. 133–137, 1980.

[9] K. Takahashi, K. Murakami, and M. Yokota, "Preparation of polycrystalline alkali halide fibers for infrared transmission," in *Tech. Dig. 1981 Spring Meeting of Soc. Appl. Phys. Japan*, p. 225, Apr. 1981.

[10] D. Chen, R. Skogman, E. G. Bernal, and C. Butter, "Fabrication of silver halide fibers by extrusion," in *Fiber Optics*, B. Bendow and S. S. Mitra, Eds. New York: Plenum, 1979, pp. 119–122.

[11] J. A. Harrington, M. Braunstein, B. Bobbs, and R. Braunstein, "Scattering losses in single and polycrystalline materials for infrared fiber applications," in *Physics of Fiber Optics*, B. Bendow and S. S. Mitra, Eds. Columbus, OH: American Ceramics Society, 1981, pp. 94–103.

[12] H. Mori and T. Izawa, "A new loss mechanism in ultralow loss optical fiber materials," *J. Appl. Phys.*, vol. 51, pp. 2270–2271, Apr. 1980.

[13] S. Sakuragi, "Polycrystalline KRS-5 infrared fibers for power transmission," in *Advances in IR Fibers, Tech. Dig. SPIE*, Los Angeles, CA, Jan. 26–28, 1982, paper 320-02.

[14] J. A. Harrington and S. Hanssen, "Infrared fiber early warning receiver," in *Advances in IR Fibers, Tech. Dig. SPIE,* Los Angeles,

CA, Jan. 26–28, 1982, paper 320-21.
[15] T. J. Bridges, J. S. Hasiak, and A. R. Strand, "Single crystal AgBr infrared optical fibers," *Opt. Lett.*, vol. 5, pp. 85–86, Mar. 1980.
[16] Y. Mimura, Y. Okamura, Y. Komazawa, and C. Ota, "Growth of fiber crystals for infrared optical waveguides," *Japan. J. Appl. Phys.*, vol. 19, pp. L269–L272, May 1980.
[17] Y. Okamura, Y. Mimura, Y. Komazawa, and C. Ota, "CsBr and CsI crystal fibers for infrared transmission," in *Paper Tech. Group OQE, IECE Japan*, Nov. 1980, pp. 25–30.
[18] M. Poulain, M. Poulain, J. Lucas, and P. Brun, "Verres fluores au tetrafluorure de zirconium proprietes optiques d'un verre dope au Nd^{3+}," *Mater. Res. Bull.*, vol. 10, pp. 243–246, 1975.
[19] S. Shibata, M. Horiguchi, K. Jinguji, S. Mitachi, K. Kanamori, and T. Manabe, "Prediction of loss minima in the infrared optical fibers," *Electron. Lett.*, vol. 17, pp. 775–777, Oct. 1981.
[20] J. R. Gannon, "Optical fiber materials for operating wavelengths longer than 2 μm," *J. Non-Cryst. Solids*, vol. 42, pp. 239–246, 1980.
[21] K. Nassau, "Material dispersion zero in infared waveguides," *Electron. Lett.*, vol. 16, pp. 924–925, Nov. 1980.
[22] L. Jeunhomme, H. Poignant, and M. Monerie, "Material dispersion evaluation in a fluoride glass," *Electron. Lett.*, vol. 17, pp. 808–809, Oct. 1981.
[23] K. Jinguji, M. Horiguchi, S. Shibata, T. Kanamori, S. Mitachi, and T. Manabe, "Material dispersion in fluoride glasses," *Electron. Lett.*, vol. 18, pp. 164–165, Feb. 1982.
[24] M. G. Drexhage, O. H. El-Bayoumi, and C. T. Moynihan, "Progress in heavy metal fluoride glasses for infrared fibers," in *Advances in IR Fibers, Tech. Dig. SPIE*, Los Angeles, CA, Jan. 1982, paper 320-06.
[25] Y. Ohishi, S. Mitachi, S. Shibata, and T. Manabe, "Impurity absorption loss due to rare earth elements in a fluoride glass," *Japan. J. Appl. Phys.*, vol. 20, pp. L191–L193, Mar. 1981.
[26] Y. Ohishi, S. Mitachi, and T. Kanamori, "Impurity absorption losses in the infrared region due to 3d transition elements in fluoride glass," *Japan. J. Appl. Phys.*, vol. 20, pp. L787–L788, Nov. 1981.
[27] S. Mitachi and T. Manabe, "Fluoride glass fiber for infared transmission," *Japan. J. Appl. Phys.*, vol. 19, pp. L313–L314, June 1980.
[28] S. Mitachi, S. Shibata, and T. Manabe, "Teflon FEP-clad fluoride glass fibre," *Electron. Lett.*, vol. 17, pp. 128–129, Feb. 1981.
[29] S. Mitachi, T. Miyashita, and T. Kanamori, "Fluoride-glass cladded optical fibres for mid-infrared ray transmission," *Electron. Lett.*, vol. 17, pp. 591–592, Aug. 1981.
[30] S. Mitachi and T. Miyashita, "Preparation of low-loss fluoride glass fibre," *Electron. Lett.*, vol. 18, pp. 170–171, Feb. 1982.
[31] T. Kanamori, S. Mitachi, T. Miyashita, and T. Manabe, "Optical attenuation of AlF_3-based fluoride glass fibers," in *Tech. Dig. on Semiconductor and Materials*, in *1981 Fall Meet. IECE Japan*, Oct. 1981, p. 369.
[32] M. G. Drexhage, B. Bendow, T. J. Loretz, J. Mansfield, and C. T. Moynihan, "Preparation of multicomponent fluoride glass fibers by single crucible technique," in *Tech. Dig. 3rd Int. Conf. on Int. Optics and Optical Fiber Commun.*, Apr. 1981, p. 32.
[33] R. J. Ginther and D. C. Tran, "Fluoride glasses for IR transmitting fibers," in *Tech. Digest 3rd Int. Conf. on Int. Optics and Optical Fiber Commun.*, Apr. 1981, p. 32.
[34] S. Shibata, Y. Terunuma, and T. Manabe, "Ge-P-S chalcogenide glass fibers," *Japan. J. Appl. Phys.*, vol. 19, pp. L603–L605, Oct. 1980.
[35] E. M. Dianov, "Materials for infrared low loss fibers," in *Advances in IR Fibers, Tech. Dig. SPIE*, Los Angeles, CA, Jan. 1982, paper 320-04.
[36] T. Miyashita and Y. Terunuma, "Optical transmission loss of As-S glass fiber in 1.0–5.5 μm wavelength region," *Japan. J. Appl. Phys.*, vol. 21, pp. L75–L76, Feb. 1982.
[37] H. Takahashi, I. Sugimoto, T. Sato, and S. Yoshida, "GeO_2-Sb_2O_3 glass optical fibers for 2–3 μm fabricated by VAD method," in *Advances in IR Fibers, Tech. Dig. SPIE*, Los Angeles, CA, Jan. 1982, paper 320-16.
[38] B. Szigeti, "Compressibility and absorption frequency of ionic crystals," *Proc. Roy. Soc. London Ser. A*, vol. A204, pp. 51–62, 1950.
[39] R. Olshansky and G. W. Scherer, "High GeO_2 optical waveguide," in *Proc. 5th ECOC and 2nd IOOC*, Amsterdam, The Netherlands, pp. 12.5-1–12.5.3, 1979.
[40] J. A. Harrington, "Crystalline infrared fibers," in *Infrared fibers (0.8–12 μm)*, *Proc. SPIE*, Los Angeles, CA, Feb. 9–13, 1981, pp. 10–15.
[41] T. Kanamori, private communication.
[42] S. Takahashi, S. Shibata, T. Kanamori, S. Mitachi, and T. Manabe, "New fluoride glasses for infrared transmission," in *Advances in Ceramics Vol. 2, Physics of Fiber Optics*, B. Bendow and S. S. Mitra, Eds. Columbus, OH: American Ceramics Society, 1981, pp. 74–82.
[43] S. Mitachi, S. Shibata, and T. Manabe, "Preparation of preforms for fluoride glass fibers," *Japan. J. Appl. Phys.*, vol. 20, pp. L337–L339, 1981.
[44] D. C. Tran, R. J. Ginther, G. H. Sigel, Jr., and K. H. Levin, "Preparation and characterization of zirconium fluoride based glass fibers," *Tech. Dig. of Topical Meet. on Optical Fiber Commun.*, Phoenix, AZ, Apr. 13–16, 1982, paper TUCC-3.
[45] K. Ohsawa, T. Shibata, K. Nakamura, and M. Kimura, "Light scattering in fluorozirconate glasses," presented at the *1st Int. Symp. on Halide and Other Nonoxide Glasses*, Cambridge, MA, Mar. 23–26, 1982.
[46] M. Matecki, M. Poulain, and M. Poulain, "Etude ves verres fluores dans les quaternaires ZnF_2-ThF_4-AlF_3-MF_2," *Mater. Res. Bull.*, vol. 16, pp. 749–757, 1981.
[47] A. R. Hilton, C. E. Jones, and M. Brau, "Non-oxide IVA-VA-VIA chalcogenide glasses," *Phys. Chem. Glass*, vol. 7, no. 4, pp. 105–112, 1966.
[48] C. A. Angell and D. C. Ziegler, "Inorganic chloride and mixed halide glasses with low maximum phonon frequencies," *Mater. Res. Bull.*, vol. 16, pp. 279–283, 1981.
[49] T. Miyashita and Y. Terunuma, unpublished.
[50] H. Poignant, J. LeMellot, and J. F. Bayon, "Fluoride glasses for infrared optical fibers," *Electron. Lett.*, vol. 17, no. 8, pp. 295–296, 1981.
[51] A. Bornstein, N. Croitoru, and E. Marom, "Chalcogenide infrared glass fibers," in *Advances in IR Fibers, Tech. Digest SPIE*, Los Angeles, CA, Jan. 26–28, 1982, paper 320-18.
[52] S. Shibata, Y. Terunuma, and T. Manabe, "Sulfide glasses fibers for infrared transmission," *Mater. Res. Bull.*, vol. 16, pp. 703–714, 1981.
[53] S. Shibata, T. Manabe, and M. Horiguchi, "Preparation of Ge-S glass fibers with reduced OH, SH content," *Japan. J. Appl. Phys.*, vol. 20, no. 1, pp. L13–L16, 1981.
[54] J. Y. Boniort, C. Brehm, PH. Dopont, D. Guignot, and C. LeSergent, "Infrared glass optical fibers for 4 to 10 micron bands," in *Proc. 6th Europ. Conf. Opt. Commun.*, pp. 61–64, Sept. 16–19, 1980.
[55] J. R. Gannon, "Materials for mid-infrared waveguides," in *Infrared fibers (0.8–12 μm)*, *Proc. SPIE*, Los Angeles, CA, Feb. 9–13, 1981, pp. 62–68.
[56] I. W. Donald and P. W. Mcmillan, "Review–Infrared transmitting materials," *J. Mater. Sci.*, vol. 13, pp. 2301–2312, 1978.
[57] A. Rosiewicz and J. R. Gannon, "Effects of irradiation on mid-infrared transmitting glass," *Electron. Lett.*, vol. 17, no. 8, pp. 184–185, 1981.
[58] M. Robinson, R. C. Pastor, R. R. Turk, D. P. Devor, M. Braunstein, and R. Braunstein, "Infrared-transparent glasses derived from the fluorides of zirconium, thorium and barium," *Mater. Res. Bull.*, vol. 15, pp. 735–742, 1980.
[59] Y. Okamura, Y. Mimura, Y. Komazawa, and C. Ota, "CsI crystalline fiber for infrared transmission," *Japan. J. Appl. Phys.*, vol. 19, no. 10, pp. L649–L651, Oct. 1980.
[60] R. R. Turk, "Rolling KCl fiber–A feasibility study," in *Advances in IR Fibers, Tech. Dig. SPIE*, Los Angeles, CA, Jan. 1982, paper 320-17.
[61] K. Jinguji, M. Horiguchi, and T. Manabe, "Spectral loss measurement system for IR optical fibers," *Appl. Opt.*, vol. 21, pp. 571–572, Feb. 1982.
[62] S. Mitachi, unpublished data.
[63] J. Lucas, "Fluoride glasses with large optical window for IR fibers," in *Advances in IR Fibers, Tech. Dig. SPIE*, Jan. 1982, paper 320-05.

[64] H. Takahashi, I. Sugimoto, and T. Sato, "Germanium oxide glasses optical fiber prepared by VAD method," *Electron. Lett.*, vol. 18, pp. 398–399, May 1982.
[65] J. A. Harrington and A. G. Standlee, "Optical attenuation in IR fibers," in *Tech. Dig. CLEO '81*, Washington, DC, June 10–12, 1981, pp. 16–17.
[66] B. Bendow, R. N. Brown, M. G. Drexhage, T. J. Loretz, and R. L. Kirk, "Material dispersion of fluorozirconate-type glasses," *Appl. Opt.*, vol. 20, pp. 3688–3690, 1981.
[67] W. S. Rodney, I. H. Malitson, and T. A. King, "Refractive index of arsenic trisulfide," *J. Opt. Soc. Amer.*, vol. 48, pp. 633–636, 1958.
[68] S. Shibata, private communication.
[69] S. H. Wemple, "Material dispersion of optical fiber," *Appl. Opt.*, vol. 18, pp. 31–35, 1979.
[70] K. Nassau, "The material dispersion zero in infrared optical waveguide materials," *Bell Syst. Tech. J.*, vol. 60, no. 3, pp. 327–337, 1981.
[71] L. Jeunhomme, "Single-mode-fiber design for 4 μm band operation," *Electron. Lett.*, vol. 17, no. 6, pp. 560–561, 1981.
[72] K. Jinguji, M. Horiguchi, S. Mitachi, T. Kanamori, and T. Manabe, "Infrared power delivery in the 2.7 μm band in fluoride glass fiber," *Japan. J. Appl. Phys.*, vol. 20, no. 6, pp. L392–L394, 1981.
[73] S. D. Allen and J. A. Harrington, "Optical absorption in KCl and NaCl at infrared laser wavelengths," *Appl. Opt.*, vol. 17, no. 11, pp. 1679–1680, June 1978.
[74] T. Oku, H. Mori, and M. Ikeda, private communication.
[75] C.K.N. Patel, "Potential and application of infrared optical fibers," in *Infrared fibers (0.8–12 μm)*, *Proc. SPIE*, Los Angeles, CA, 1981, pp. 22–30.
[76] G. Tangonan, A. G. Pastor, and R. C. Pastor, "Single crystal KCl fibers for 10.6 μm integrated optics," *Appl. Opt.*, vol. 12, no. 6, pp. 1110–1111, 1973.
[77] D. L. Wood and J. Tauc, "Weak absorption tails in amorphous semiconductors," *Phys. Rev. B*, vol. 5, no. 8, pp. 3144–3151, 1972.
[78] D. C. Tran, R. C. Ginther, and G. H. Sigel, Jr., private communication.

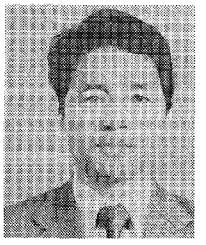

Tadashi Miyashita was born in Hokkaido, Japan, in 1943. He received the B.S. and the M.S. degrees in physics from Hokkaido University, Sapporo, Japan, in 1966 and 1968, respectively, and the Ph.D. degree in the area of optical fiber technology from the Tokyo Institute of Technology, Tokyo, Japan, in 1980.

He joined Ibaraki Electrical Communication Laboratory, Nippon Telegraph and Telephone Public Corporation, Tokai, Ibaraki, Japan, in 1968, and has been engaged in research on dielectrics. Since 1971, he has been engaged in the developmental research on the optical fiber fabrication techniques and their characteristics including both silica-based and nonsilica-based glass fibers for infrared transmission.

Dr. Miyashita is a member of the Japan Society of Applied Physics and the Institute of Electronics and Communication Engineers of Japan.

Toyotaka Manabe was born in Hokkaido, Japan, in 1942. He received the B.E., M.E., and Dr.E. degrees in electronics from Hokkaido University, Sapporo, Japan, in 1964, 1966, and 1978, respectively.

He joined the Ibaraki Electrical Communication Laboratory, Nippon Telegraph and Telephone Public Corporation, Tokai, Ibaraki, Japan, in 1966, and studied oxide magnetic materials and rapid quenching techniques. Since 1979, he has been engaged in research on infrared optical glass fibers.

Dr. Manabe is a member of the Physical Society of Japan and the Institute of Electronics and Communication Engineers of Japan.